CLIMATE AND PREDICTABILITY OF ALASKA WILDFIRES

By

Peter A. Bieniek

RECOMMENDED: _____

_____

_____

_____
Advisory Committee Chair

_____
Chair, Atmospheric Sciences Program

APPROVED: _____
Dean, College of Natural Science and Mathematics

_____
Dean of the Graduate School

_____
Date

CLIMATE AND PREDICTABILITY OF ALASKA WILDFIRES

A

THESIS

Presented to the Faculty

of the University of Alaska Fairbanks

in Partial Fulfillment of the Requirements

for the Degree of

MASTER OF SCIENCE

By

Peter A. Bieniek, B.S.

Fairbanks, Alaska

December 2007

Abstract

Wildfires burn an average of 3,760km^2 each year in Alaska, but varies greatly from year to year. These fires, started by human and natural causes, can endanger life and property when they approach populated areas. The relationship between seasonal area burned and monthly and seasonal average mean sea level pressure, surface air temperature, total column precipitable water, 500hPa and 700hPa geopotential height, 700hPa specific humidity and 1000-500hPa layer thickness is examined. The assessment was done by examining the spring and summer seasonal composites associated with extreme high and low seasons. This showed the predominant anomalies from the climatology for seasons of both extremes. Point correlations were also made between seasonal area burned and the aforementioned climate variables for the entire Northern Hemisphere. Points of particularly high correlation with area burned were used in multiple regressions for both spring and summer, and for the preseason only to predict seasonal area burned. Results show correlations of about 0.78 for the preseason regression and 0.91 for the total period. The seasonal area burned in Alaska is intimately linked with the ongoing synoptic situation on monthly and seasonal scales before and during the fire season.

Table of Contents

Page

Page

List of Figures

Page

Page

Page

List of Tables

Page

List of Appendices

Page

Acknowledgements

I would like to first thank my advisors Gerd Wendler and Martha Shulski who have both contributed greatly to my research and who are both responsible for my being able to do this work at all. Special thanks are also due to the members of my committee Uma Bhatt and Nicole Mölders for their helpful comments. Blake Moore for the two graphics he provided. Thanks to all of the members of the Atmospheric Science Group at the University of Alaska Fairbanks who create a wonderful and stimulating work environment. I owe much gratitude to my parents, family, and friends for each of their critical roles in helping me get to this point in my life. I should also thank the generations of people who have helped make Alaska what it is today, a place that I greatly admire and have wanted to live for most of my life. It is indeed a great honor to have been able to do this research and I am grateful to have received such an opportunity. Finally, special thanks to the State of Alaska and the Alaska Climate Research Center who funded this research.

Chapter 1 Introduction

Wildfires throughout the world play an important role in air quality, climate, ecosystems, economy, and in many aspects of human life. Alaska, despite its high latitudinal location, experiences the global fire rite yearly with approximately 3,760km^2 area burned annually on average. Each summer, these wildfires can endanger life and property if they approach populated areas while at the same time playing an important natural role in the ecosystems of Alaska. The landscape and climate of the Interior makes it the prime area where the majority of wildfires occur in the state. Additionally, the climate has influence over the relative strength of a fire season in terms of the total area burned during the fire season. In this chapter, we will examine the reasons why wildfire occurs in Alaska and then look at the influence of weather and climate on wildfire and its application to Alaska.

1.1 Wildfire in Alaska

Wildfires have been present as an important factor in the ecosystem of the boreal forests of Alaska for thousands of years burning during both wet and dry climatic periods (Lynch et al. 2004). Kasischke et al. (2002) observed that 96% of all wildfires in Alaska occur in the Interior portion of the state. Kasischke et al. (2002) showed furthermore that 76% of these wildfires occur during a period of the summer from the beginning of June to about mid-July. During years of high wildfire occurrence, wildfires occur at much greater frequency and burn later in the season. Kasischke et al. (2002) additionally

observed that 73% of the area burned during the period 1950-1999 occurred during only ten seasons of high wildfire activity.

Climatologically, Alaska is a region of extremes throughout the year. Alaska features a maritime climate type in the southern portion of the state with continental climate in Interior Alaska and an Arctic climate type in the northern portion of the state (Searby 1968). It is primarily in the continental climate of Interior Alaska where most wildfires occur (Figure 1.1). Moisture transport from the Pacific Ocean into Interior Alaska is hindered greatly by the presence of the Alaska Range, which spans a great distance orientated east to west across much of the southern part of the state marking the southern boundary of the Interior. The Brooks Range makes the northern boundary of the Interior just north of the Arctic Circle.

The continental climate of the Interior summer season features high temperatures with relatively low precipitation amounts. Fairbanks, an example of an Interior location, has a mean maximum temperature of 21.6 C in June, 22.8 C in July, which decreases to 17.2 C in August. In extreme cases, daily high temperatures have risen as high as 37.8 C (Fort Yukon) during the summer in the Interior. Mean precipitation in Fairbanks in June is 35.6mm, 43.9mm in July, and 44.2mm in August. In the southern portion of the state there tends to be more precipitation than in the Interior during summer, for example Valdez on the southern coast receives an average precipitation 76.5mm in June, over twice the mean of Fairbanks. The arctic climate of the northern portion of the state features climatologically drier conditions than the Interior, however temperatures are much colder along the coast than in the Interior during the summer; Barrow reports only

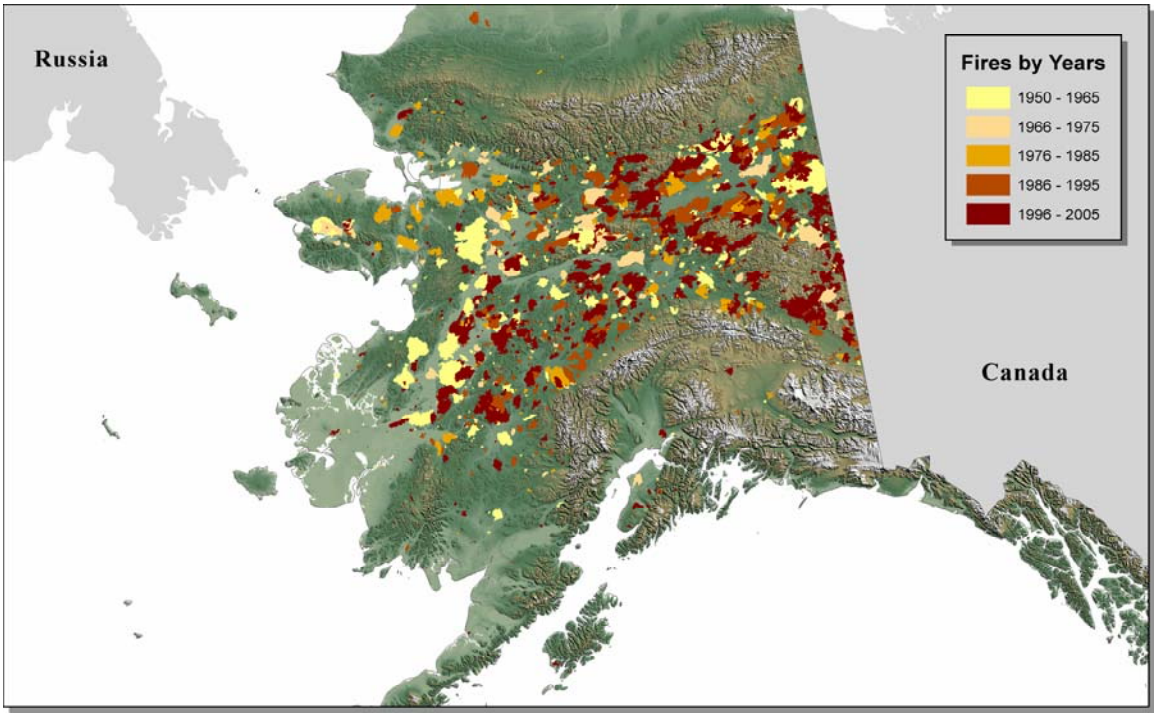

Figure 1.1 Alaska fire history 1950-2005. Courtesy of Blake Moore, Alaska Climate Research Center (personal correspondence).

8.2mm of precipitation on average in June with a mean maximum temperature of only 4.2 C (http://climate.gi.alaska.edu).

Lightning occurrence in Alaska is tied to landscape and elevation (Reap 1991, Dissing and Verbyla 2003). With an average of over 32,400 strikes per year (McGuiney et al. 2005), lightning ignition of wildfires in Alaska accounts for only 24% of wildfire ignitions; despite this, lightning caused fires are responsible for about 80% of the total area burned based on analysis of wildfire statistics for Alaska from 1950 to 1969 (Barney 1971). Sullivan (1963) found that much of this lightning is due to low-level convergence caused by thermal troughs, which are often found in the continental climate of the Interior during the summer months. About 90% of all lightning incidence occurs in the months of June and July and is generally confined to the afternoon hours in Interior Alaska (Reap 1991).

The environmental effects of Alaska wildfires were discussed by Chambers and Chapin (2002) who showed that for burned black spruce there is an overall reduction in the net radiation by as much as 80W/m^2 during the midday hours. The water balance and energy balance are altered for newly burned areas (Mölders and Kramm 2007) and along with altering the surface roughness, mesoscale circulations in the vicinity of the fire scar can occur. Mölders and Kramm (2007) further showed that models predict an increase in cloudiness and alteration in the type of hydrometeors present in these clouds besides causing a general increase in surface temperature by 3 C in the vicinity of burn scars, especially for those of larger size.

Due to low population density, not all wildfires that start in Alaska are suppressed by human intervention. Various types of fire management have been devised which allow some wildfires to burn out on their own without suppression activities. This fact has resulted in several different types of fire management options generally associated with the population density of the geographic area. Examples of fire management options available in the State of Alaska for the 2007 fire season are shown in Figure 1.2. Fire management techniques have been shown to be effective in Alaska by reducing the total seasonal area burned (DeWilde and Chapin 2006).

Wildfires in Alaska also have impacts on the climate by releasing trace gases into the atmosphere. During years with particularly intense wildfire activity, emissions can reach as high as 38Tg of carbon (French et al. 2003). Emissions from Alaska wildfires can also be transported long distances. In 2004, emissions from wildfires burning in Alaska and the neighboring Yukon Territory were transported across Canada to Wisconsin (Damoah et al. 2006) and to Nova Scotia with a transport time of 8-10 days (Duck et al. 2007).

1.2 Weather, Climate and Wildfires

There exists an important relationship between weather, climate, and wildfires. Synoptic scale weather conditions that lead to wildfire start and spread usually only last for a few days. In general terms, the critical elements generally associated with fire weather are wind, temperature, humidity, and precipitation according to Pyne et al. (1996). Schroeder et al. (1964) found relationships between synoptic scale weather

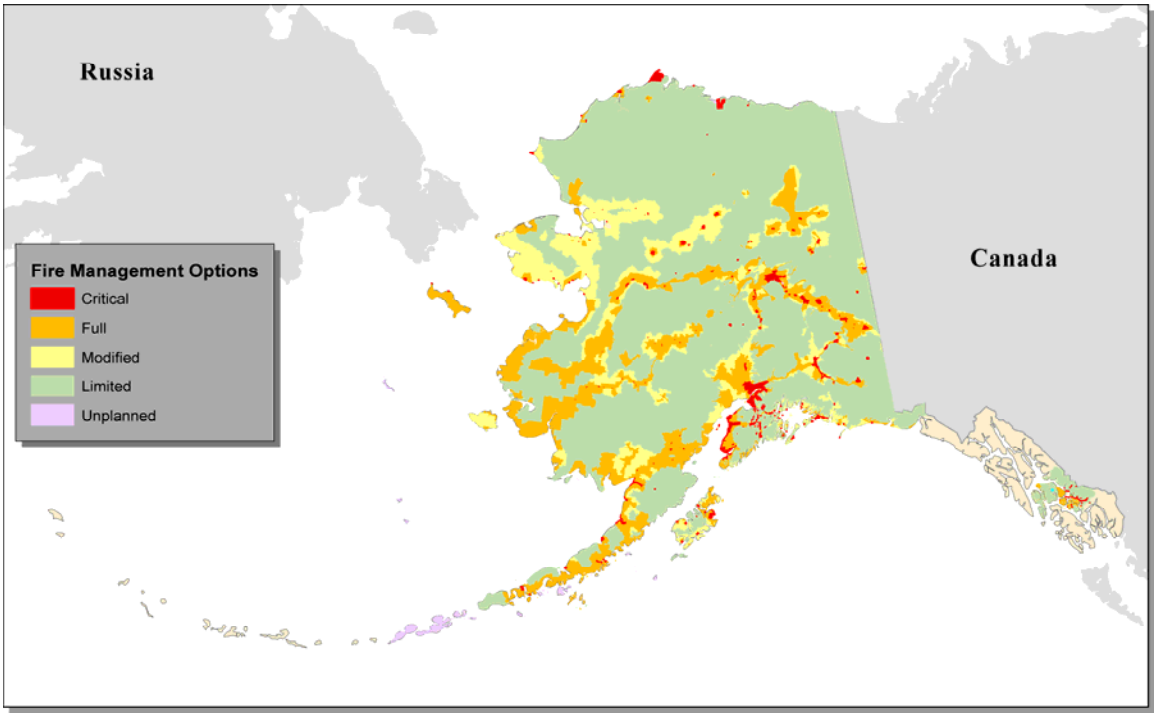

Figure 1.2 Map of fire management regions for Alaska. Courtesy of Blake Moore, Alaska Climate Research Center (personal correspondence).

conditions and wildfire activity during fire seasons in different regions of the United States. Increased wildfire activity was found to be associated with surface frontal boundaries and 500hPa shortwave troughs (Brotak and Reifsnyder 1977) and with jet streams (Schaefer 1957) in the USA. While these shorter term weather conditions are known to be associated with circumstances that lead to wildfires, there has also been considerable work done that shows relationships between climate, in the form of anomalies and teleconnection indices, and wildfires on a variety of monthly and seasonal scales.

The relationships between wildfires and climate scale atmospheric conditions have been examined extensively. Relationships between monthly averaged climate variables and monthly area burned were found for areas of Canada during the period 1953-1980 (Flannigan and Harrington 1987). It was additionally found that there are statistically significant correlations between 500hPa geopotential height anomalies and area burned in Canada, and the patterns associated with high and low area burned years were identified (Skinner et al. 1999, 2001).

The interaction of teleconnection indices with wildfires has also been revealed on a variety of seasonal scales and for different locations of North America and the Pacific Ocean (Johnson and Wowchuck 1992, Hess et al. 2001, Chu et al. 2002, Duffy et al. 2005, Touret et al. 2006). Associations between atmospheric climate anomalies and wildfires have also been identified for other geographic regions for a range of short and long time scales (Johnson and Wowchuck 1992, Hostetler et al. 2005, Pereira et al. 2005).

Henry (1978) found that correlations exist between wildfire and occurrence in Alaska considering 500hPa geopotential height synoptic map types. The author identified 500hPa geopotential height patterns associated with lightning caused wildfires and human caused forest fires in Alaska. These patterns were then applied to make predictions of wildfire occurrence for specific days. Hess et al. (2001) examined the impact of El Nino on wildfires in Alaska. The authors revealed that 15 out of 17 of the years that were identified as having extreme high wildfire incidence occurred during El Nino years.

Besides El Nino, other teleconnections have also been identified as important for Alaska fire seasons. The Pacific Decadal Oscillation (PDO) and the East Pacific (EP) pattern were shown to be related to seasonal wildfire occurrence considering the 1950 to 2003 period (Duffy et al., 2005). Fauria and Johnson (2006) found that the Pacific Decadal Oscillation, the El Nino Southern Oscillation, and the Arctic Oscillation all interact to affect lightning caused wildfire occurrence in Alaska and Canada.

Statistical prediction of area burned has been shown to be effective for wildfires in many areas of the world (Duffy et al. 2005, Westerling et al. 2001, 2003, Pereira et al. 2005). Using multiple regression techniques, Duffy et al. (2005) showed that it is possible to predict and diagnose the seasonal area burned in Alaska based on climate indices such as the PDO and EP along with air temperature and precipitation spanning several months, including the preseason. The authors succeeded in fitting the seasonal area burned considering only eight predictors that explained 79% of the variance of the response variable, area burned. This study showed that given careful selection of climate

data for use as predictors, it is possible to predict the magnitude of the Alaska fire season in advance within some level of uncertainty.

1.3 Objectives

For this study, the relationship between the atmosphere and the area burned in Alaska and atmospheric variables, their location in the Northern Hemisphere, and time of year they occur is examined and quantified in detail. Information gained from this study can be used to not only determine a climatology associated with years of extreme high or low area burned, but can also be applied in an objective statistical prediction of the area burned using only preseason conditions thus eliminating the need for variables to be included that require prediction themselves. This eliminates some of the added uncertainty associated with the prediction. A seasonal climatology is also developed for years with extreme high and low area burned considering the same climate variables.

Monthly average climate variables considered for this study were 500hPa geopotential height, 700hPa geopotential height, 700hPa specific humidity, 1000-500hPa layer thickness, total column precipitable water, and surface air temperature. These variables were selected for examination so that both the middle and lower troposphere would both be considered as possible locations of predictors of the area burned in Alaska.

Chapter 2 Data and Methods

2.1 Data

2.1.1 Alaska Area Burned

Data of total seasonal area burned for Alaska was obtained from the Alaska Fire Service, which maintains the large-fire database for Alaska. The Alaska Fire Service compiles this data set by totaling the area burned by wildfire in the state for each year. This data set does not distinguish between wildfires that were ignited by lightning or by human or other causes, and spans the years 1955-2005. The data also does not differentiate whether or not wildfires where suppressed. All geographic regions of the state are also considered within this data set. Fire size is determined from a combination of ground surveys, airborne surveys, aerial photographs, and, for the later part of the time series, from satellite imagery of the burned area.

The area burned dataset (Figure 2.1) has a yearly average area burned of 3,755km^2 with a median of 1,578km^2. In view of the fact that this dataset has a skewness of 2.3, this data most certainly does not follow a Gaussian distribution as is true with many environmental data sets. Most of the total area burned occurs during the years with extreme high area burned. The most area burned in a single season occurred in 2004 with 26,165km^2 total area burned. By contrast, the year with the smallest area burned (1964) had a total area burned of only 14km^2. This gives a total range of 26,151km^2 for the area burned dataset. In the period of 1955-2005 there was a total area burned of 191,505km^2 in Alaska.

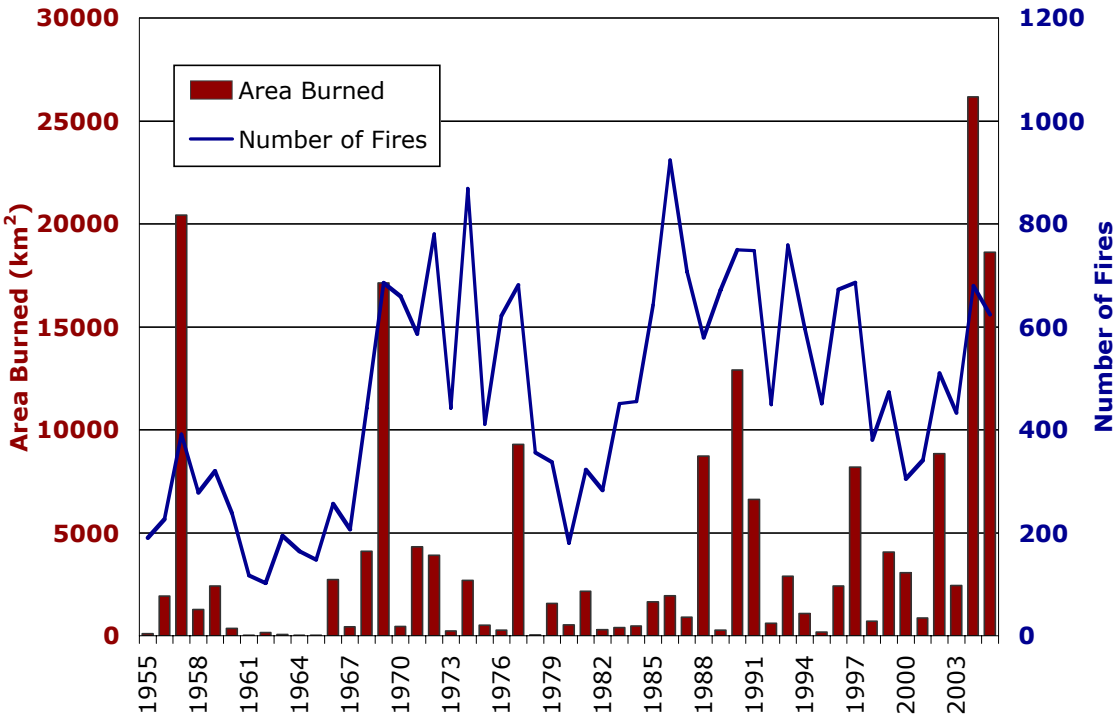

Figure 2.1 Total seasonal area burned and number of fires.

2.1.2 Reanalysis Data

Data for the climate variables were obtained from the National Centers for Environmental Prediction and National Center for Atmospheric Research (NCEP/NCAR) Reanalysis Project (Kalnay et al. 1996, http://www.cdc.noaa.gov/cdc/reanalysis/). The monthly averages and long term mean climatologies of 500hPa geopotential height, 700hPa geopotential height, 700hPa specific humidity, total column precipitable water, 1000-500hPa layer thickness, and surface air temperature for the entire Northern Hemisphere for the time period 1955-2005 were retrieved. The long term mean climatology used is for the period 1968-1996 as specified by the NCEP/NCAR Reanalysis. The data are gridded with a resolution of 2.5 degree grid spacing. This gives a total of 37 grid points from the equator to the North Pole by 144 grid points in the longitudinal direction giving a total of 5328 grid points considered in the Northern Hemisphere.

2.2 Methods

2.2.1 Selection of Extreme Years

Considering the area burned dataset, the years 1955-2005 were ranked in order of total seasonal area burned (Table 2.1). Statistical examination of the dataset revealed that the top five years with the most extreme area burned area were statistically extreme outliers and makes up the top 10% of the dataset. There were no outliers on the low end of the area burned, nevertheless, the bottom 10% were selected as years with extreme low area burned. The analysis identified the extreme high years as having an average area

Table 2.1 Years with extreme high and low area burned.

High Years		Low Years	
Year	Area Burned (km^2)	Year	Area Burned (km^2)
1957	20435.3	1961	20.6
1969	17125.6	1964	13.9
1990	12905.7	1965	28.7
2004	26165.8	1978	31.4
2005	18615.5		

burned of 19,050km^2 and the extreme low years an average area burned of around 24km^2. The total area burned in the years ranked as the top five highest makes up 49% of the total area burned during the 1955-2005 period. The four years ranked as the extreme low years make up less than 0.1% of the total area burned during the same period.

2.2.2 Composite Anomalies

Previous work outlined in the introduction has shown relationships between composite seasonal anomalies in climate variables and area burned in Alaska; seasonal composite anomalies in regard to the years with high and low extreme area burned were computed.

The years ranked as the high extreme years were first considered, and the seasonal composites of monthly average climate variables: 500hPa geopotential height, 700hPa geopotential height, 700hPa specific humidity, total column precipitable water, 1000-500hPa mean layer thickness, and surface air temperature for the spring season (March April May hereafter MAM) and summer season (June July August hereafter JJA) were plotted. The long term mean climatology was then subtracted from each of the seasonal composites calculated. The result is a seasonal composite anomaly field for MAM and JJA for each climate variable.

The student t-test was then employed to compute the significance level of the differences of the means of the high extreme years from the climatology. We consider p-values of 0.05 to be significant for the purposes of this study. The identical procedure was preformed for the extreme low area burned years.

2.2.3 Selection of Predictors

Selection of climate variables for predictors proved to be one of the most difficult components of this study. Potential predictors were selected from the monthly average 500hPa geopotential height, 700hPa geopotential height, 700hPa specific humidity, total column precipitable water, 1000-500hPa mean layer thickness, and surface air temperature fields for the Northern Hemisphere. In this case, the months March through August were all considered as sources of potential predictors. This process was carried out to include the climatic conditions ongoing during the summer fire season while also examining the climate situation one season before the fire season itself.

The first step in the selection of predictors was to determine where in the monthly average fields of each of the predictors the best relationships with seasonal area burned in the form of a correlation coefficient that is statistically significant at the 0.05 level. This objective was accomplished by computing the correlation that the time series associated with each grid point in the Northern Hemisphere has with the seasonal area burned in Alaska. This procedure was completed for each month for each individual climate variable. This results in correlation fields for each month in the period March through August for each climate variable.

By means of these fields of monthly point correlations, a procedure was then devised to group points of high correlation together. This procedure consisted of searching the entire grid for points with correlation greater than 0.5 or less than -0.5. With these points identified, all points within 10-15 degrees latitude and longitude of one another were then grouped together. This procedure was then used for all of the fields of

each climate variable and for each month. Some degree of subjectivity was necessary at this point because it would not always be clear if two areas of high correlation were spatially attached to one another based on visual inspection. This complexity resulted in somewhat arbitrary decisions being made if a large area of significantly high correlations had two or more distinct peaks.

It was necessary to determine a point to represent each area of high correlation that was identified by the procedure outlined above. The point with the highest correlation coefficient in each group was selected to represent the area of high correlation. This provided for one or more potential predictors for each month for each climate variable. This procedure alone resulted in 57 potential predictors, which is a very high number considering that there are only 51 years of area burned data that were used for the fitting. Consequently, a subjective selection of predictors based on their proximity to study area of Alaska considering what month the predictor occurred in (i.e. preseason predictors can be farther away from Alaska than those occurring during the summer) was used to reduce the total number of predictors. This subjective selection served as an excellent first step in the predictor screening process. In the end, the subjective screening resulted in the final set of 23 potential predictors that were considered for the multiple regressions that will be discussed in subsequent sections.

2.2.4 Multiple Regression

As a method of relating climate variables to the Alaska fire season, multiple regression analysis has proven useful for previous studies (Duffy et al. 2005). Only the

predictors found by the selection procedure outlined in the previous section were considered in the calculation. The first step of the procedure was to fit all of the potential predictors together using a multiple regression. The equation of the regression is of the form:

$$Y = a_1*x_1 + a_2*x_2 + \ldots + a_n*x_n + b \quad (2.1)$$

Where a_1, a_2, a_n and b are coefficients that are determined by least squares regression and x_1, x_2, and x_n are the input values of the predictors. Equation 2.1 results in a value Y, which is predicted area burned for this study.

The t-value was determined for each predictor to determine whether or not its coefficient was significantly different from zero. A backwards elimination scheme was then employed which consisted of removing the predictor with the least significant t-value. The multiple regression is then refitted each time and each time the least significant variable was removed. Variables were only removed by this method and not according to any other method of removal. This iterative procedure stopped when all predictors in multiple regression were significant at the 0.05 significance level. This procedure was completed twice, first considering all potential predictors, and then considering only those potential predictors in the preseason defined as March and April as the fire season generally starts in May.

2.2.5 Cross-validation and Assessment

To determine the overall stability of the final multiple regression models presented in the previous section, the models must be able to predict the area burned for

fire seasons not considered in the original fitting. If the model is useful as a prediction tool, then when it is fitted considering a shortened time period it should be able to predict similar results as the original model that considered the full time period. The procedure used for the cross-validation in this instance was to fit the multiple regression with data only for the period 1955-1990 and then use the fitting equation from this to predict the area burned for the years 1991-2005. Then a comparison was made between the two fittings, which gives information on the performance of the model and whether or not it can be used for years not considered in the fitting as a forecast tool. This procedure was followed for both the total season and for the fitting that considered only the preseason predictors.

The multiple regression is examined to assess the overall accuracy of predicting area burned for different classes of observed area burned. Examining the frequency distribution of the observed area burned data is the first step of the procedure. The bin sizes are then adjusted until there are an equal number of cases in each bin. For this study, four bins were used. The procedure then continues by taking the area burned data that was predicted by the multiple regression for each year and then placing it in the appropriate bin. Each year off the observed data set also is given the identical treatment. Now, for each bin that the observed data was in, we can observe the percent of years that were predicted in the correct bin, and the percent predicted in the three other bins.

Chapter 3 Results

3.1 Seasonal Composite Anomalies

3.1.1 MAM Extreme High Years

Composite 500hPa geopotential height anomalies for MAM show a positive anomaly of approximately 50m over all Alaska (Figure 3.1). This anomaly is significant at the p=0.05 level. In addition to the positive anomaly observed over Alaska, a significant negative anomaly of approximately 40m is present over northwestern Russia. Other negative and positive anomalies are present in the Atlantic Ocean and in the Pacific Ocean, but are not statically significant.

The 1000-500hPa layer thickness composite anomalies (Figure 3.2) show a positive anomaly of similar shape to that of the 500hPa geopotential height and 700hPa geopotential height (not shown) anomalies for the same time period. This anomaly is significant at the p=0.05 level, however the anomaly centered over northwestern Russia, which is also present in this anomaly field, is not statistically significant. There is a larger area of the tropical Pacific that is significant, but with a much smaller anomaly in magnitude than what is present farther north.

Composite anomalies of mean sea level pressure (Figure 3.3) show, most notably, a significant anomaly of approximately -3hPa over the northern Pacific Ocean and the Kamchatka Peninsula of Russia with a secondary significant anomaly of similar magnitude over northwestern Russia. No significant positive anomalies are present in this anomaly field.

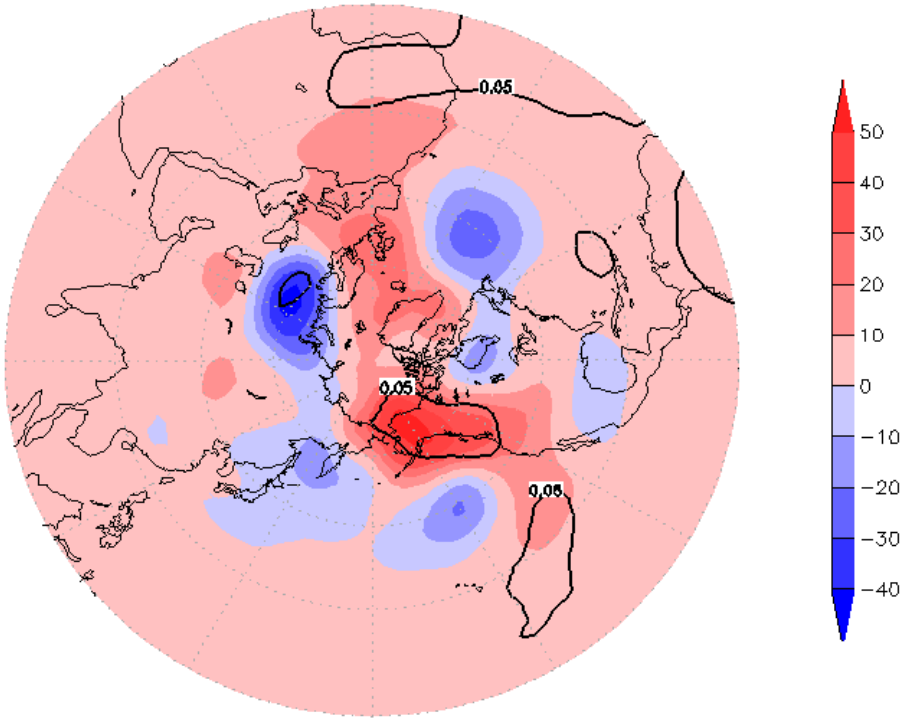

Figure 3.1 MAM 500hPa geopotential height seasonal composite anomalies (m) for years with extreme high area burned. Areas of significant anomalies p=0.05 contoured.

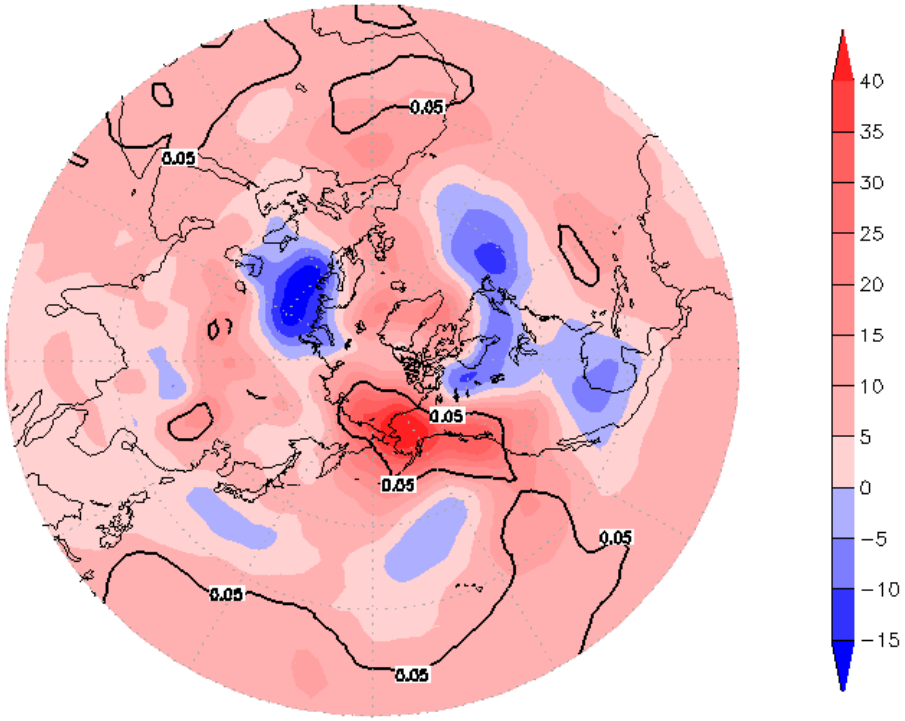

Figure 3.2 MAM 1000-500hPa layer thickness composite anomalies (m) for years with extreme high area burned. Areas of significant p=0.05 anomalies contoured.

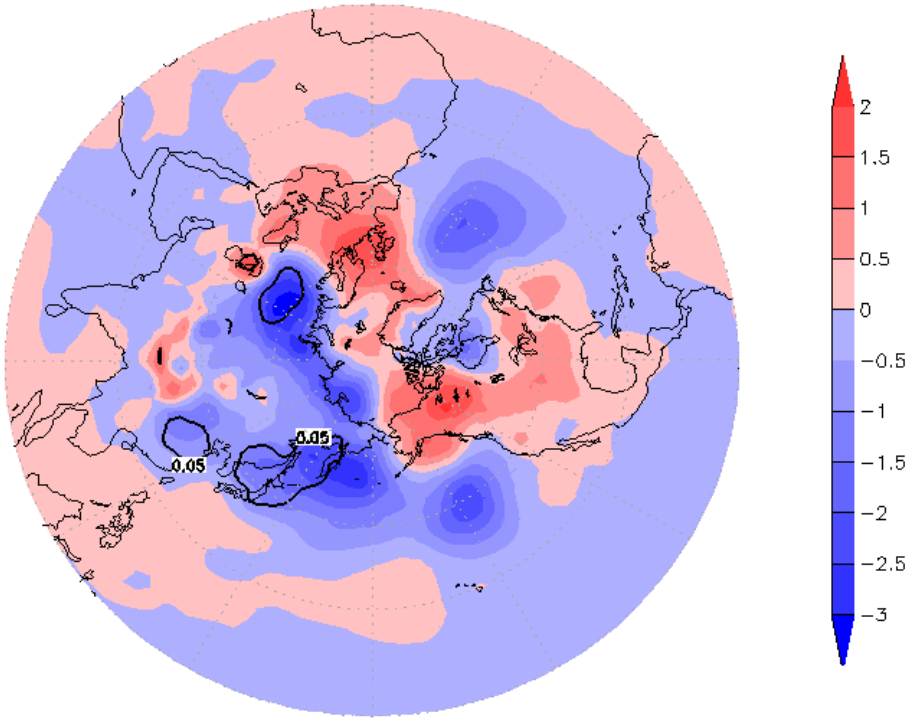

Figure 3.3 MAM mean sea level pressure composite anomalies (hPa) for years with extreme high area burned. Areas of significant p=0.05 anomalies contoured.

Total column precipitable water composite anomalies (Figure 3.4) show lower latitudes primarily as having widespread significant anomalies, however, these anomalies tend to cover much smaller areas than the anomalies in the 500hPa geopotential height, 1000-500hPa layer thickness and mean sea level pressure fields. Significant positive anomalies are also present around and including Alaska and into the North Pacific and Arctic Oceans. An equivalent pattern to the precipitable water anomalies occurs in the 700hPa specific humidity composite anomaly fields (not shown).

MAM composite anomalies for surface air temperature show one primary, positive anomaly over the Arctic Ocean northeast of Russia (Figure 3.5). This anomaly is significant at the p=0.05 level and has a central magnitude of greater than 3.5 C. The negative anomaly situated over northwest Russia is not statistically significant.

3.1.2 JJA Extreme High Years

Composite seasonal anomalies for the JJA season for 500hPa geopotential height (Figure 3.6) show two notable and statistically significant positive anomalies. The first anomaly is situated over much of western Alaska and centered over the Bering Sea. The second positive anomaly is centered over northern Greenland and covering a larger area than the anomaly over Alaska. The 700hPa geopotential anomaly fields show a nearly identical pattern (not shown).

The 1000-500hPa layer thickness anomalies (Figure 3.7) show a very similar pattern to the 500hPa geopotential height anomaly field (Figure 3.6). The primary difference is that the anomaly over Alaska is of greater magnitude than the anomaly.

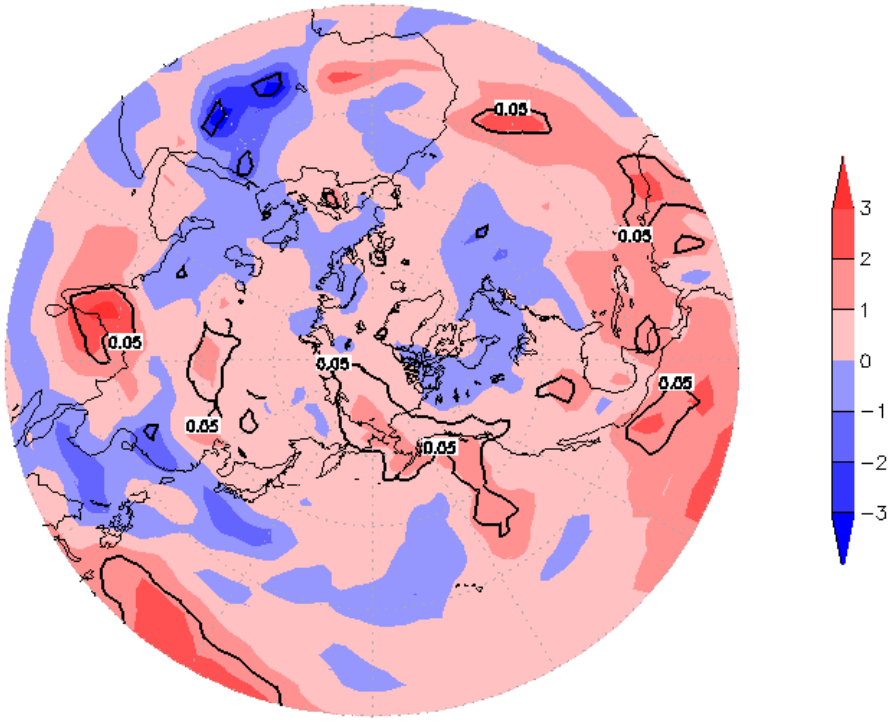

Figure 3.4 MAM total column precipitable water composite anomalies (kg/m^2) for years with extreme high area burned. Areas of significant p=0.05 anomalies contoured.

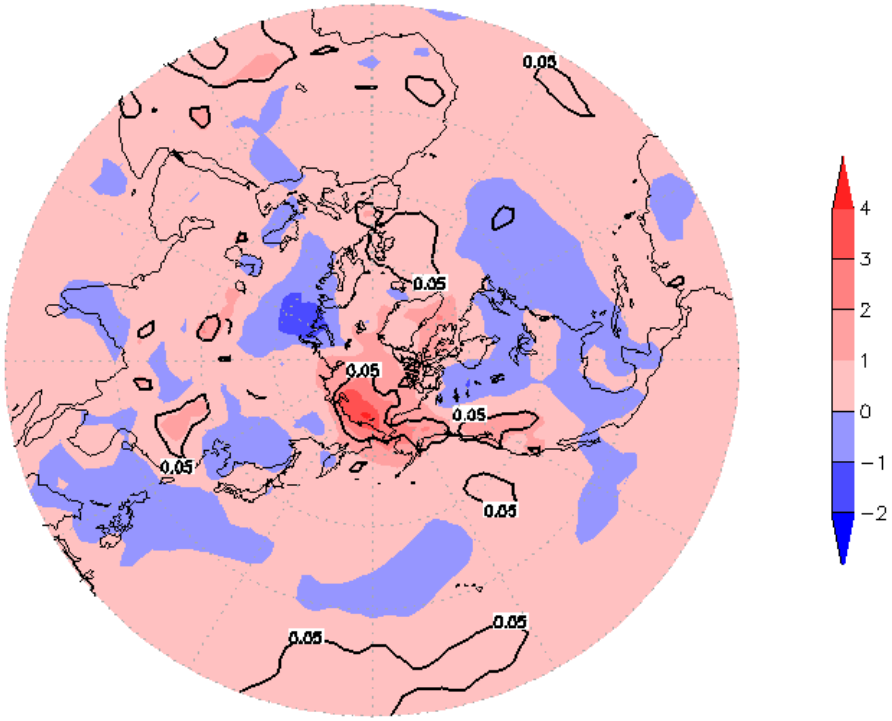

Figure 3.5 MAM surface air temperature composite anomalies (C) for years with extreme high area burned. Areas of significant p=0.05 anomalies contoured.

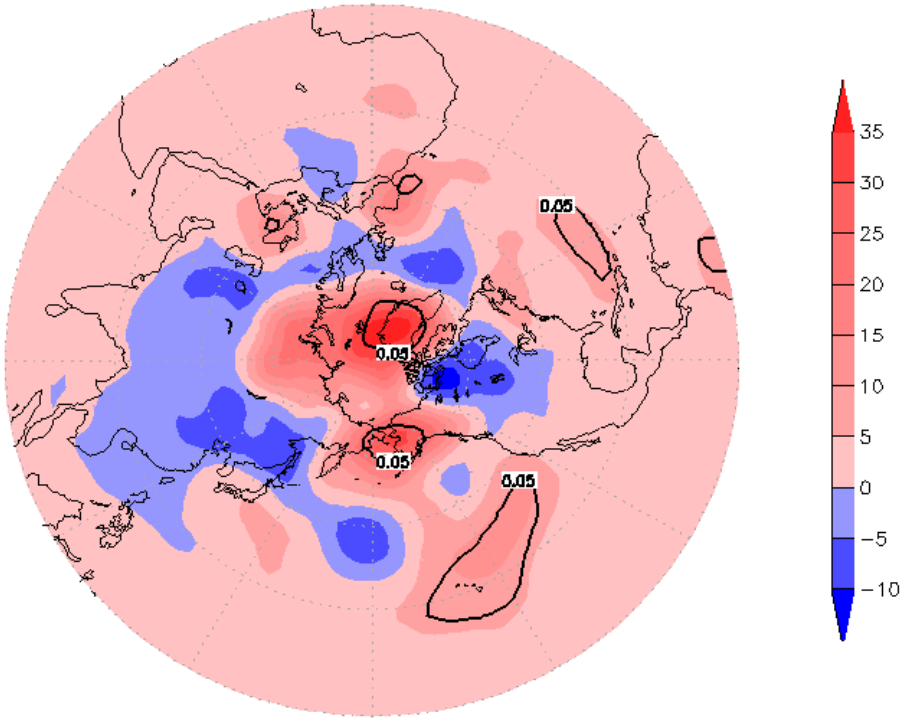

Figure 3.6 JJA 500hPa geopotential height composite anomalies (m) for years with extreme high area burned. Areas of significant p=0.05 anomalies contoured.

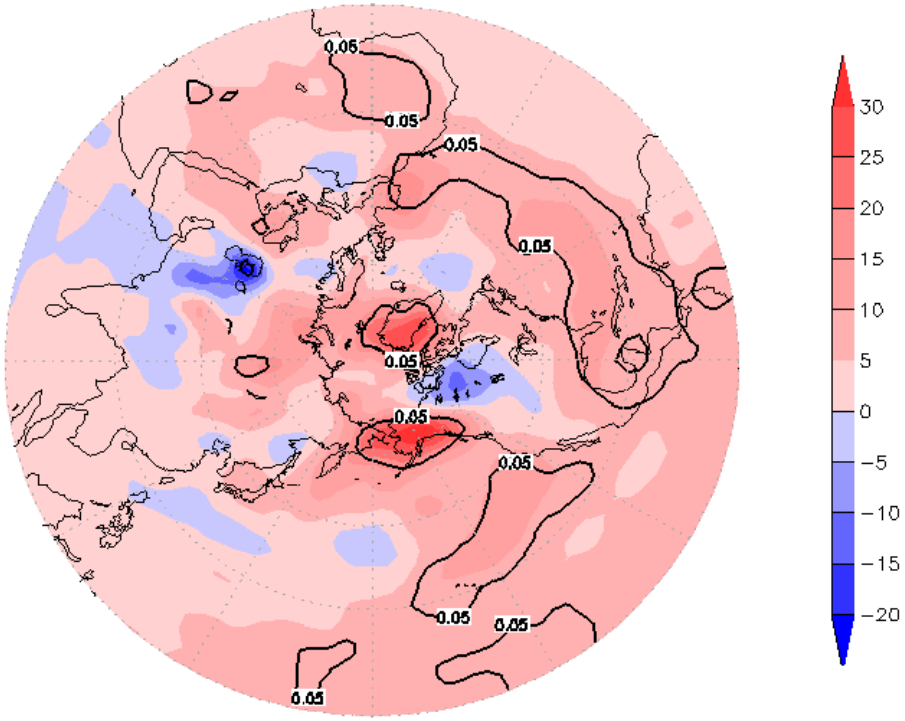

Figure 3.7 JJA 1000-500hPa layer thickness composite anomalies (m) for years with extreme high area burned. Areas of significant p=0.05 anomalies contoured.

present over Greenland. Both anomalies are statistically significant. It is also worth noting that there is a much greater geographical area that is statistically significant for this anomaly pattern. Many of these significant areas are off of the west coast of the United States in the Pacific Ocean and also in an area of the Atlantic Ocean starting in the Gulf of Mexico and stretching to the Straits of Gibraltar

Surface air temperature anomalies for extreme high years (Figure 3.8) show a significant positive anomaly situated roughly over eastern Alaska stretching into much of southern and Interior Alaska and including part of western Yukon Territory. A second positive anomaly is again present over northern portions of Greenland. Additional significant regions include the Gulf of Alaska stretching south along the western coast of North America. Significant regions for surface air temperature anomalies also are present in the Pacific Ocean around the Equator and in portions of the Atlantic Ocean in the vicinity of the northwestern coast of Africa. A negative anomaly is situated east of Alaska over northern Canada, however this anomaly is not statistically significant.

The moisture fields of 700hPa specific humidity and total column precipitable water show areas of high significance, however no discernable anomaly pattern in relation to Alaska is present (not shown). Mean sea level pressure composite seasonal anomalies, while showing a strong positive anomaly over much of the Arctic, do not show any anomalies of note that are significant so the mean sea level pressure anomalies are not presented.

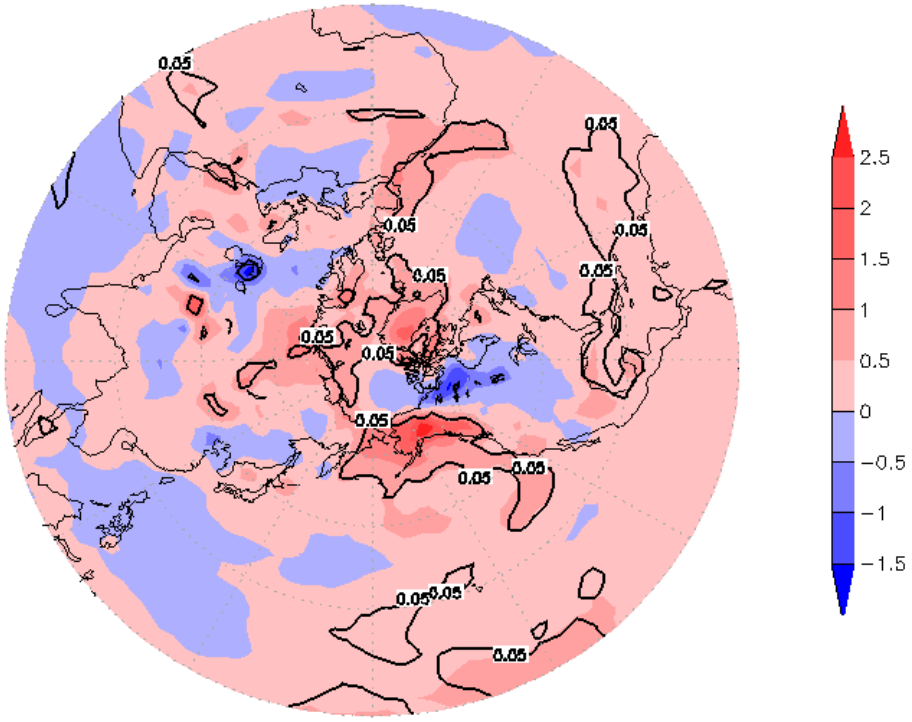

Figure 3.8 JJA surface air temperature composite anomalies (C) for years with extreme high area burned. Areas of significant p=0.05 anomalies contoured.

3.1.3 MAM Extreme Low Years

The composite anomalies for total column precipitable water (Figure 3.9) show a pronounced positive anomaly situated in northern Africa. Throughout much of the rest of the Northern Hemisphere there are very few anomalies, and none compare in magnitude to the African anomaly. A similar situation is also present for the 700hPa specific humidity composite anomalies (not shown).

Composite anomalies for 500hPa goepotential height, 700hPa geopotential height, 1000-500hPa layer thickness, and mean sea level pressure all show similar anomaly and significance patterns therefore the former only will be shown. 500hPa goepotential height anomalies (Figure 3.10) show a positive anomaly that is statistically significant and situated in the Gulf of Alaska. An additional positive anomaly that is significant is also present in the Atlantic Ocean near the north west coast of Africa. Significant negative anomalies are present over portions of western Russia and in the North Atlantic. Widespread significant, although much weaker, negative anomalies can be observed in portions of northern Africa and across much of Asia and stretching into portions of the Pacific Ocean.

Surface air temperature composite anomalies (Figure 3.11) show areas of significant negative anomalies over much of the Arctic Ocean north of Alaska and Siberia. Areas of significant positive anomalies are generally located farther south over areas of Asia and Africa.

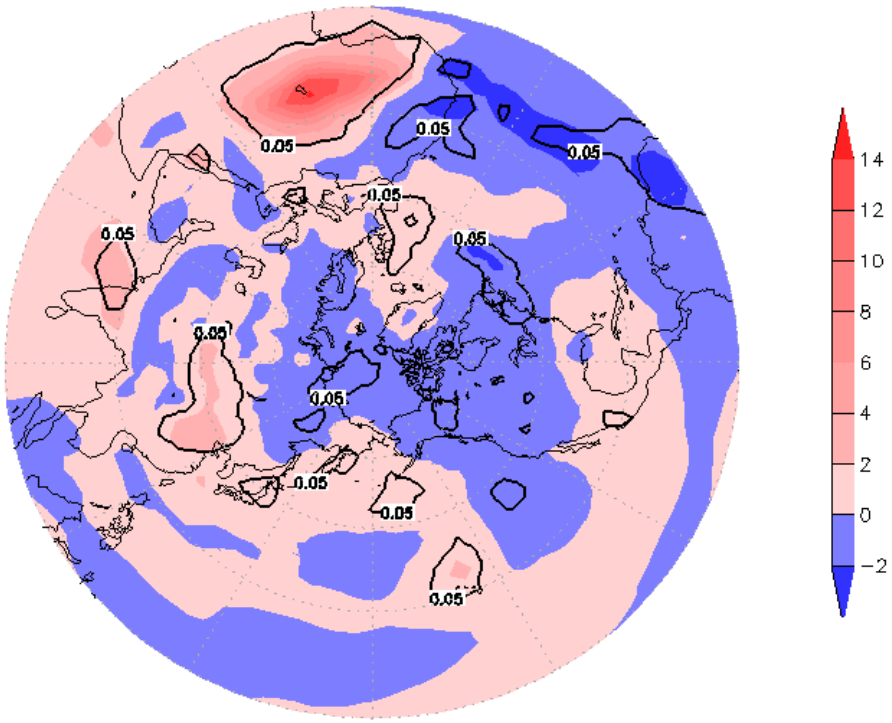

Figure 3.9 MAM total column precipitable water composite anomalies (kg/m^2) for years with extreme low area burned. Areas of significant p=0.05 anomalies contoured.

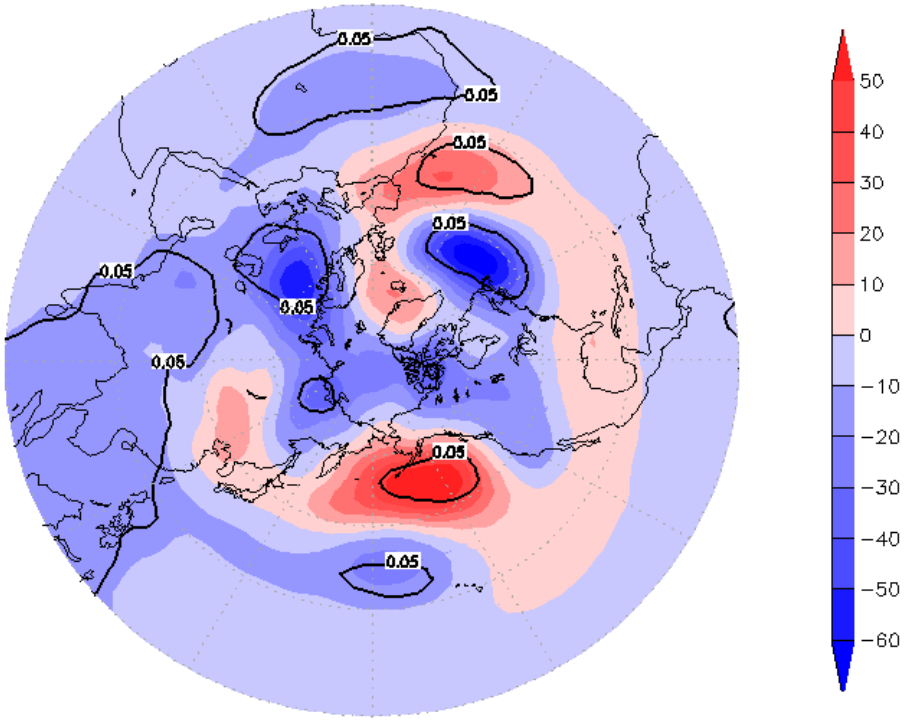

Figure 3.10 MAM 500hPa geopotential height composite anomalies (m) for years with extreme low area burned. Areas of significant p=0.05 anomalies contoured.

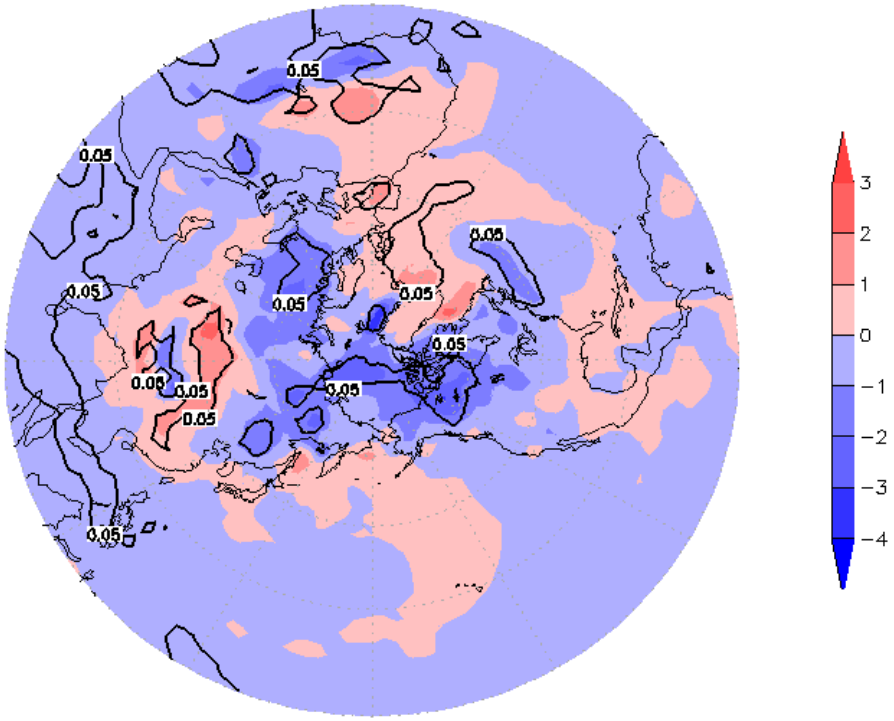

Figure 3.11 MAM surface air temperature composite anomalies (C) for years with extreme low area burned. Areas of significant p=0.05 anomalies contoured.

3.1.4 JJA Extreme Low Years

Much like for the MAM extreme low years, total column precipitable water and 700hPa specific humidity composite anomalies both show a statistically significant anomaly over Saharan Africa (Figure 3.12). The rest of the Northern Hemisphere shows either no anomalies or a few negative anomalies that are significant at lower latitudes over the oceans. Surface air temperature anomalies (Figure 3.13) show a negative anomaly over northern Africa in the vicinity of the pronounced positive anomaly in the total column precipitable water fields for the same season (Figure 3.12). The 1000-500hPa layer thickness anomalies (Figure 3.14) display similar behavior to the surface air temperature anomalies with the exception that there is no negative anomaly present in North Africa.

The composite 500hPa geopotential height anomalies field (Figure 3.15) shows a positive anomaly present over much of the Arctic Ocean north of Russia. A significant negative anomaly is present over the United Kingdom in addition to the negative anomaly over far eastern Russia. A large area of the Northern Hemisphere encompassing portions of the subtropics, the entire tropical region and much of Asia and Africa is statistically significant. The positive anomaly north of Siberia over the Arctic Ocean is also statistically significant at the 0.05 level. This pattern is nearly identical lower in the atmosphere for the 700hPa geopotential height composite seasonal anomalies (not shown). Although reduced in extent, the composite anomalies of mean sea level pressure

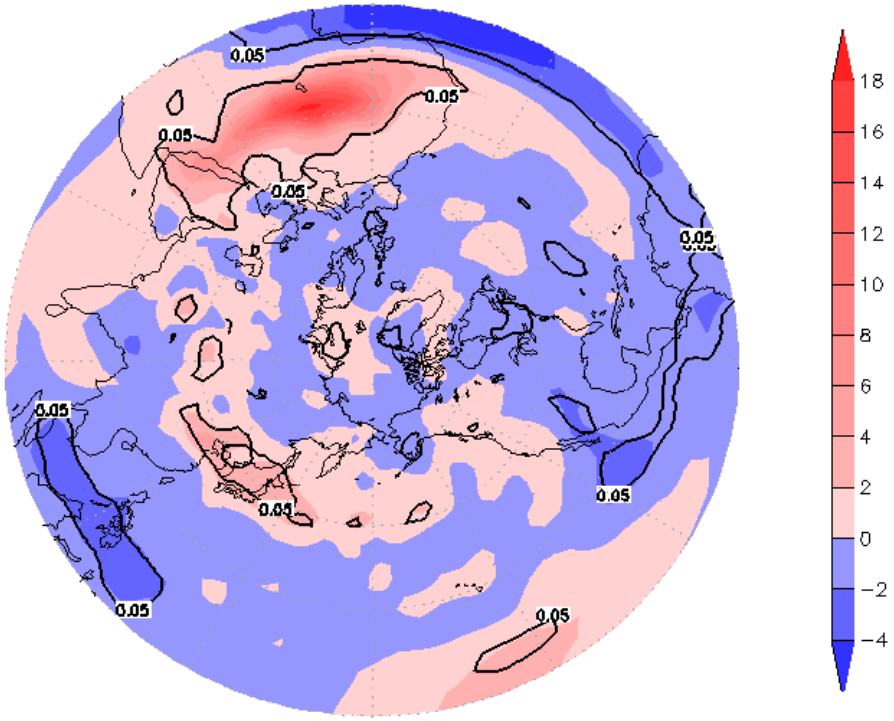

Figure 3.12 JJA total column precipitable water composite anomalies (kg/m^2) for years with extreme low area burned. Areas of significant p=0.05 anomalies contoured.

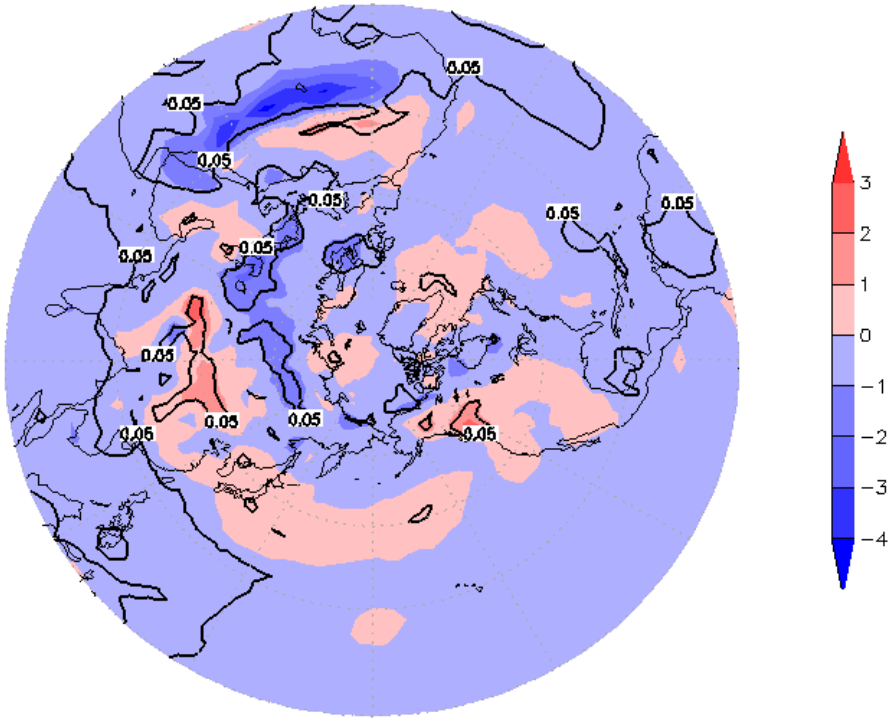

Figure 3.13 JJA surface air temperature composite anomalies (C) for years with extreme low area burned. Areas of significant p=0.05 anomalies contoured.

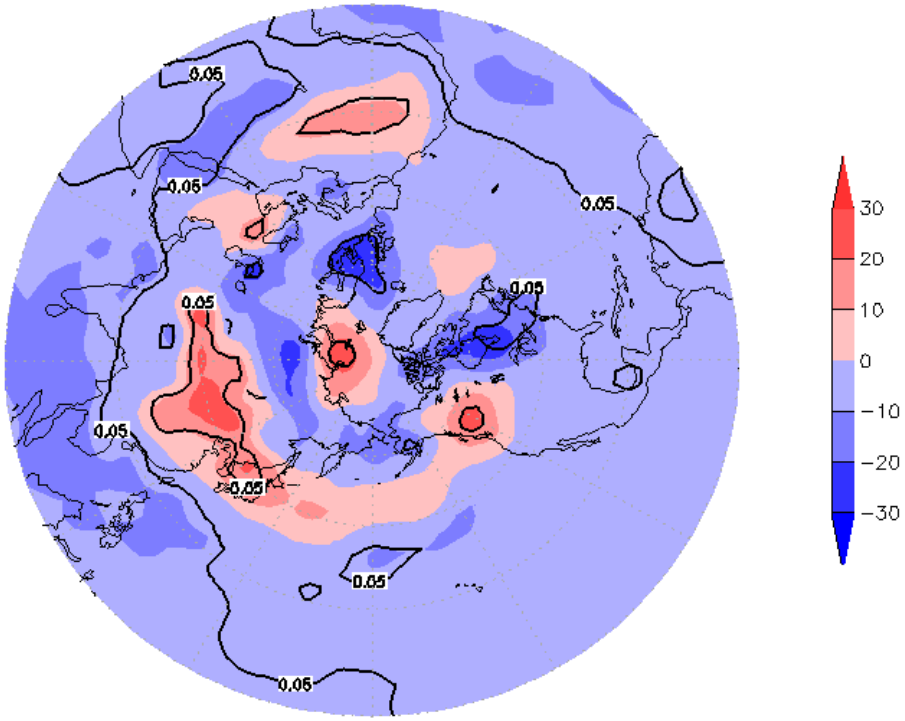

Figure 3.14 JJA 1000-500hPa layer thickness composite anomalies (m) for years with extreme low area burned. Areas of significant p=0.05 anomalies contoured.

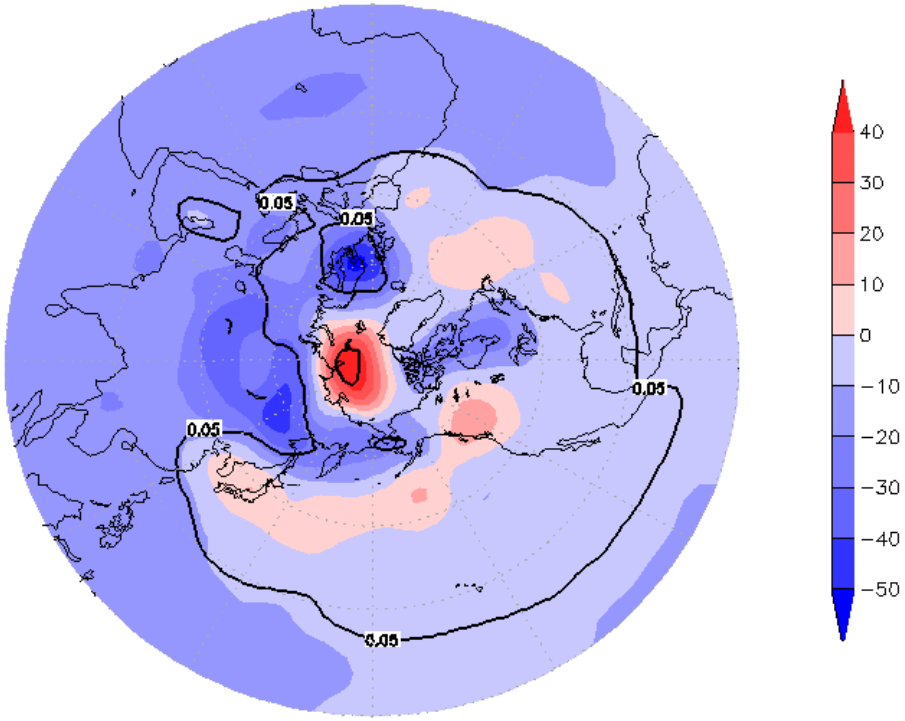

Figure 3.15 JJA 500hPa geopotential height composite anomalies (m) for years with extreme low area burned. Areas of significant p=0.05 anomalies contoured.

also show a similar pattern of anomalies as the 500hPa geopotetnial height anomaly field. The primary difference is a slight reduction in the area of extent of the significant anomalies in the tropical regions especially in the tropical Pacific Ocean.

3.2 Multiple Regression

3.2.1 Spring and Summer

The predictor selection process resulted in final a set of 23 potential predictors (Table 3.1). Potential predictors were identified for each of the months March through August. Most potential predictors were present in the May and June period. All climate variables had potential predictors identified across several months with the notable exception of mean sea level pressure which had no points selected to be part of the final set of potential predictors. The climate variables selected as potential predictors were largely moisture or temperature related and only three of the potential predictors were geopotential height.

The backwards elimination scheme identified and eliminated 13 of the potential predictors as not making a significant contribution to the multiple regression fitting when considering both preseason and season potential predictors. The multiple regression procedure resulted in a final multiple regression equation

$$Y = 5.98E+06*X_5 - 1.48E+05*X_6 + 2.18E+06*X_9 + 5.39E+05*X_{12} - 2.4E+04*X_{13} - 1.89E+04*X_{16} + 2.76E+05*X_{18} + 4.91E+05*X_{19} + 5.23E+05*X_{22} + 2.21E+04*X_{23} + 3.17E+07 \quad (3.1)$$

Which has coefficients from the remaining ten predictors (Table 3.2) and has follows the same form as Equation 2.1. The ten predictors were located from April through August

Table 3.1 List of potential predictors used for the multiple regressions.

Variable Number	Month	Latitude (N)	Longitude (E)	Variable Type
1	3	37.5	85	500 hPa HGT
2	3	35	72.5	700 hPa HGT
3	3	7.5	147.5	Thickness
4	3	2.5	142.5	Air Temperature
5	4	75	165	700 hPa Q
6	4	72.5	165	Air Temperature
7	4	75	167.5	Total Precp Water
8	5	57.5	202.5	700 hPa Q
9	5	77.5	112.5	700 hPa Q
10	5	77.5	140	Air Temperature
11	5	77.5	115	Total Precp Water
12	5	57.5	202.5	Total Precp Water
13	5	60	215	Thickness
14	5	85	305	Thickness
15	6	65	205	500 hPa HGT
16	6	65	205	700 hPa HGT
17	6	62.5	207.5	700 hPa Q
18	6	62.5	202.5	Air Temperature
19	6	62.5	205	Total Precp Water
20	6	62.5	210	Thickness
21	7	65	187.5	Air Temperature
22	8	62.5	187.5	Air Temperature
23	8	35	182.5	Thickness

Table 3.2 Statistical output for the spring and summer multiple regression. Multiple regression outputs total seasonal area burned in acres.

Variable Number	Coefficient	Standard Error	t value	p value
Intercept	3.17E+07	6.20E+07	0.511	6.12E-01
5	5.98E+06	1.63E+06	3.658	7.34E-04
6	-1.48E+05	6.92E+04	-2.145	3.81E-02
9	2.18E+06	1.02E+06	2.148	3.79E-02
12	5.39E+05	1.43E+05	3.754	5.53E-04
13	-2.40E+04	6.76E+03	-3.549	1.01E-03
16	-1.89E+04	6.97E+03	-2.718	9.66E-03
18	2.76E+05	9.88E+04	2.796	7.92E-03
19	4.91E+05	1.18E+05	4.148	1.70E-04
22	5.23E+05	1.30E+05	4.030	2.43E-04
23	2.21E+04	1.03E+04	2.136	3.89E-02
F stat: 21.02, p value: 6.53E-13				
R: 0.92, R^2: 0.84				

with all potential predictors in March having been eliminated. 500hPa geopotential height was completely eliminated in the screening process, however all of the other climate variables that were present in the potential predictor set were also still represented in the final set of predictors.

The final predictor set was largely found in the May and June period with two predictors in April and only one predictor in July and one in August. With the exception of the solitary predictor in August being located in the central Pacific Ocean, the predictors were all located either directly over Alaska, or farther west over the Arctic Ocean northeast of Siberia.

The multiple regression presented here is based on the final ten predictors outlined in the paragraphs above. When these final predictors where fitted with the area burned data for Alaska, it was found that the fitting had a correlation coefficient of 0.92 with seasonal area burned for Alaska (Table 3.2). This means that these ten predictors explain 84% of the variance of the response variable, area burned. It is important to note that the fitting identifies all of the years with extreme high area burned and follows the general observed area burned quite well (Figure 3.16). Likewise, the fitting identifies years with rather small area burned with only a few instances where the prediction was for much higher area burned when low area burned was actually observed. Due to the fact that the multiple regression equation does not account for the physical nature of area burned and no transformations were used on the data input or output, there are negative area burned output in the fitting. It appears that for all of the years shown in the fitting

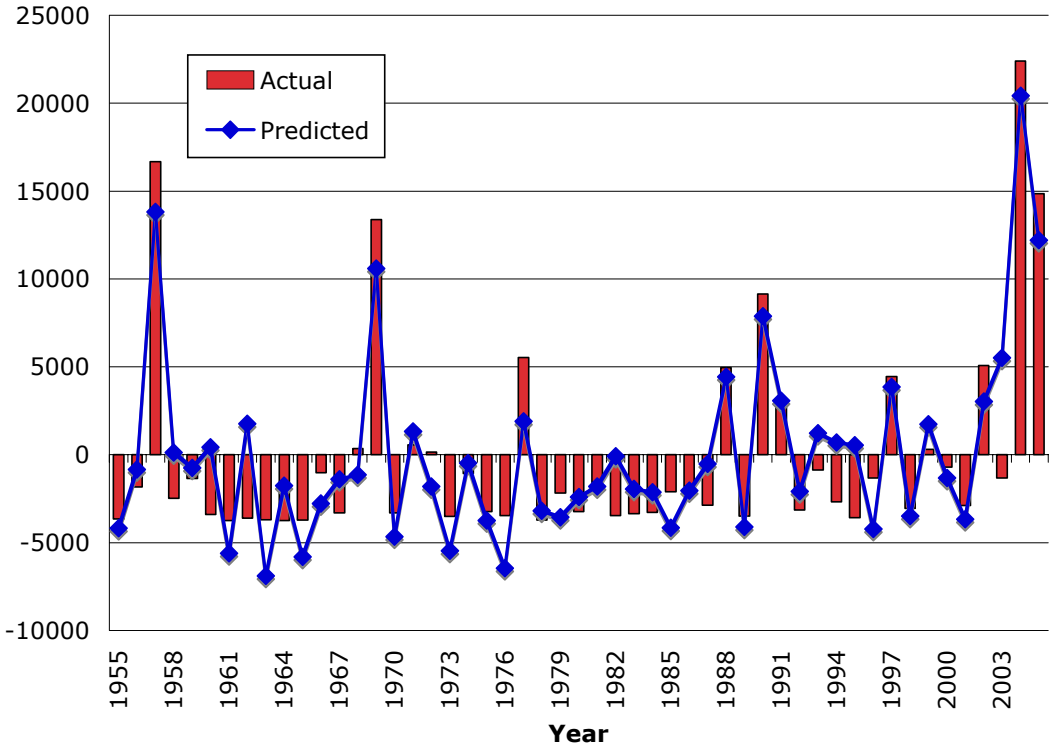

Figure 3.16 Results of the spring and summer multiple regression plotted as departure from average area burned. Blue line is the results of the multiple regression and solid red columns are the observed area burned.

with negative area burned predicted, there was small observed area burned. If the ten years that had a prediction of negative area burned are changed to zero area burned, the correlation with the observed data increased slightly to 0.93.

A cross-validation of this multiple regression was also completed as outlined in the previous methods section. This showed that when the last 15 years are removed from the fitting, very similar results are found when compared to the original fitting that used all of the data (Figure 3.17). Of high importance is that the extreme high area burned seasons of 2004 and 2005 are both identified even without using the atmospheric data for the fitting. This demonstrates that this model can identify years with extreme high area burned when used as a forecast or diagnostic tool. Overall there is a correlation of 0.97 between the model considering the full time period and the cross-validation model.

Examination of the ability of the spring and summer multiple regression to predict area burned in each of the different ranges or bins of area burned showed that the highest percentage of predictions falling in the correct category was for bin 4,050-28,330km^2 (Table 3.3) which represents the cases of extreme high area burned. The lowest number of correct instances was for when bin 370-1,620km^2 was observed, the regression in this case tends to predict area burned in bin one or bin three in this case. Bins 0-370km^2 and 1,620-4,050km^2 both had a correct prediction for about 50% of the cases with the other three bins about evenly spread accounting for the remainder of predictions.

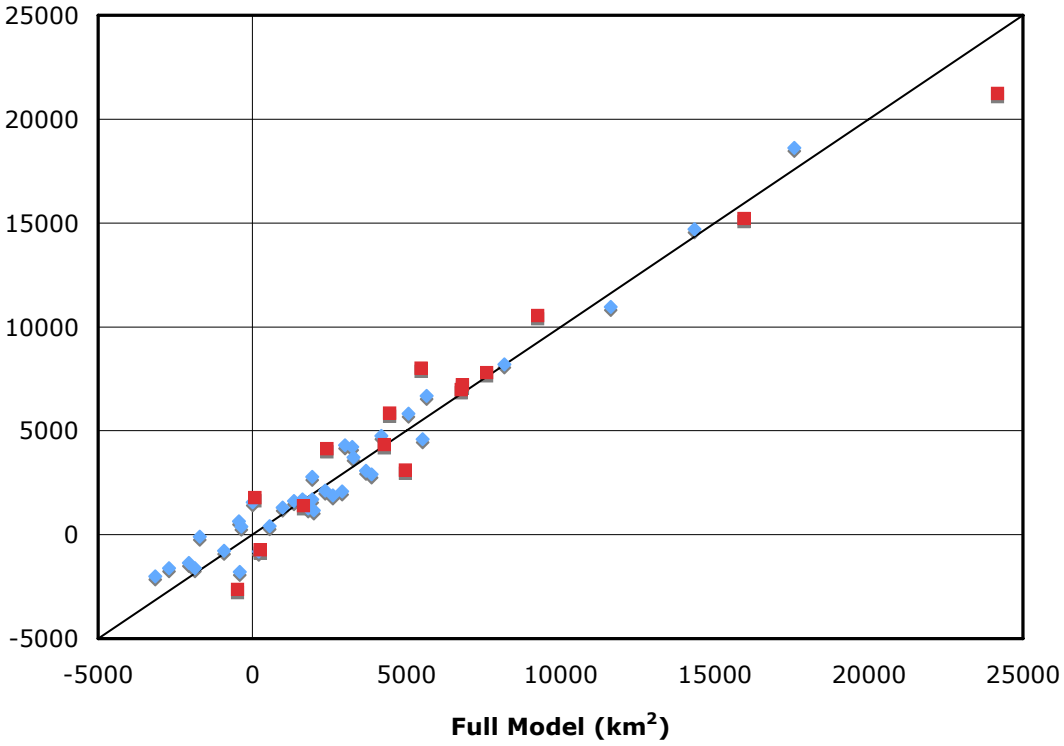

Figure 3.17 Full model versus the model fitted 1955-1990 (blue diamonds) and predicted 1991-2005 (red squares) for the spring and summer multiple regression.

Table 3.3 Accuracy of model when predicting for ranges of area burned. The vertical column of bins is of observed area burned and the horizontal bins are the predicted bins.

Bins (km^2)	0-370	370-1620	1620-4050	4050-28330
0-370	0.54	0.08	0.15	0.23
370-1620	0.38	0.08	0.46	0.08
1620-4050	0.17	0.08	0.58	0.17
4050-28330	0.00	0.00	0.08	0.92

3.2.2 Preseason

There were seven potential predictors in the preseason period of March and April, which make up 32% of the total number of predictors in the overall set of potential predictors. These predictors were generally the farthest physical distance from the study region of Alaska than any of the predictors in the summer months. Three of the potential predictors were located in the Arctic Ocean northeast of Russia. Two out of three of the geopotential height climate variables are also present during these two months with both located near the northern tip of India. Finally, in March 500hPa geopotential height and 1000-500hPa layer thickness were potential predictors, both being located in the Pacific Ocean near the Equator.

The preseason-only set of potential predictors was reduced by four in the backwards elimination process. The backward elimination procedure resulted in only three predictors being selected as significantly contributing to the multiple regression fitting (Table 3.4) and resulted in the multiple regression equation

$$Y = 2.04E+04*X_1 + 5.65E+04*X_3 + 7.99E+05*X_7 - 4.43E+08 \qquad (3.2)$$

which is of the same form as Equation 2.1. March contains two predictors considered in this fitting. One is 500hPa geopotential height at the northernmost tip of India. The second predictor is 1000-500hPa layer thickness, which is located north of New Guinea in the Pacific Ocean. The third predictor selected was the April total column precipitable water located northeast of Siberia over the Arctic Ocean.

The correlation between the fitting based on the three preseason predictors and the observed area burned is 0.78 which implies that these three preseason predictors can be

used to explain 61% of the variability of seasonal area burned (Table 3.4). On examination of the comparison of the observed and the fitted (Figure 3.18), it can be seen that the fitted data captures most of the extreme high years. When compared with the multiple regression that considered all predictors, it appears that the preseason regression does not predict as high area burned when an extreme high year was observed. There were also a few instances of the preseason fitting indicating high area burned when a smaller area was burned for that season.

As in the case of the total season multiple regression, no attempt was made to stop the multiple regression fitting from producing negative area burned predictions. As the fitting equation is not constrained by the physical nature of area burned, there are several instances when negative area burned was predicted. In most cases, negative area burned was only shown for years with fairly low observed area burned. If all seven years that the multiple regression predicted negative area burned are changed to zero, the correlation with the observed data is increased to 0.81.

Cross-validation of the preseason multiple regression showed promising results. The fitted data considering the full time period and the fitted and predicted data considering the removal of the last 15 years of the data showed an overall correlation of 0.98 (Figure 3.19). Of high practical importance, the 2004 and 2005 extreme high years are both predicted by the cross validation model. Removal of some of the time series has little impact on the quality of the prediction when considering the predictors used.

The analysis of the preseason only prediction data (Table 3.5) showed that bin 4,050-28,330km^2 had 85% predicted correctly, the highest percentage of correct

Table 3.4 Statistical output for March-April multiple regression. Multiple regression outputs total seasonal area burned in acres.

Variable Number	Coefficient	Standard Error	t value	p value
Intercept	-4.43E+08	1.03E+08	-4.289	8.87E-05
1	2.04E+04	6.41E+03	3.179	2.61E-03
3	5.65E+04	1.90E+04	2.970	4.67E-03
7	7.99E+05	1.79E+05	4.464	5.01E-05
F stat: 24.76, p value: 9.31E-10				
R: 0.78, R^2: 0.61				

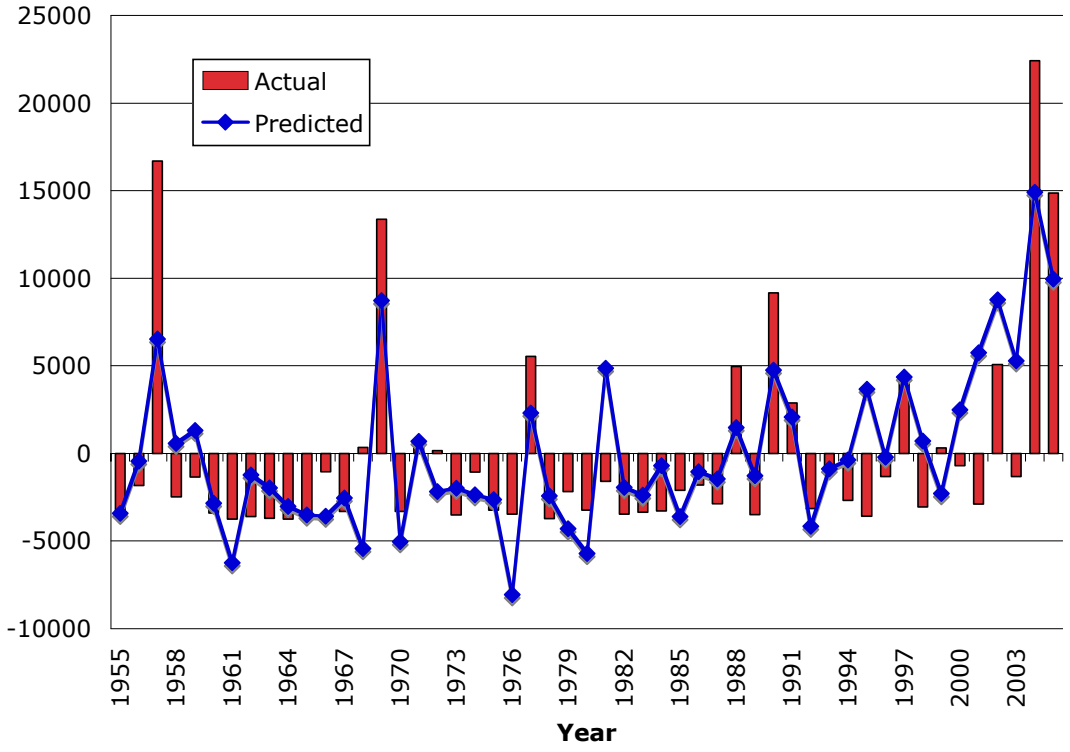

Figure 3.18 Results of the preseason multiple regression plotted as departure from average area burned. Blue line is the results of the multiple regression and solid red columns are the observed area burned.

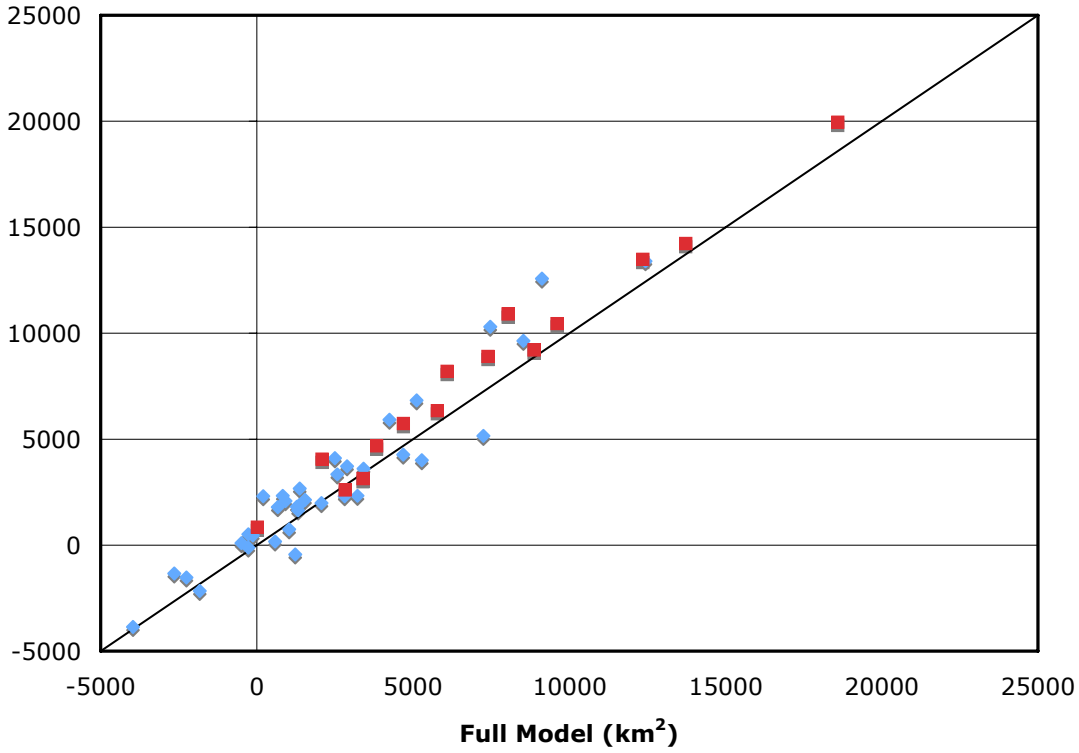

Figure 3.19 Full model versus the model fitted 1955-1990 (blue diamonds) and 1991-2005 (red squares) predicted for the preseason multiple regression.

Table 3.5 Accuracy of model prediction for ranges of area burned. The vertical column of bins is of observed area burned and the horizontal bins are the bins the predicted area burned were in.

Bins (km^2)	0-370	370-1620	1620-4050	4050-28330
0-370	0.31	0.23	0.38	0.08
370-1620	0.31	0.23	0.23	0.23
1620-4050	0.17	0.17	0.33	0.33
4050-28330	0.08	0.08	0.00	0.85

predictions. When bin 0-370km^2 was the observed bin, the multiple regression predicted most of the area burned in bins 0-370km^2, 370-1,620km^2, and 1,620-4,050km^2 relatively evenly. When bin 370-1,620km^2 was the correct bin, there were only a slightly higher number of correct predictions with the other three bins spread evenly. When bin 1,620-4,050km^2 was the correct bin, the multiple regression predicted about 33% of the cases correctly with the second most frequent prediction in this case falling into bin 4,050-28,330km^2.

Chapter 4 Discussion

The investigation of monthly and seasonal average climate variables reveal significant links between the prevailing climate during the Alaska fire season and the total seasonal area burned. The analysis showed further that the climate during the preseason also plays an important role in the overall magnitude of the area burned. Considering the results of the previous studies concerning the relationships between climate and wildfire activity outlined in the introduction that showed similar relationships in Alaska and in other regions of the world, these results are expected. Perhaps the most important results presented in the previous section are that there are major differences in the climate situations for years with extreme high and low area burned and that there are areas of significant correlation with seasonal area burned and climate variables when considering all fire seasons in the period 1955-2005. Through the use of a multiple regression, the seasonal area burned can be predicted using only climate variables.

4.1 Climatology of Extreme Years

Seasonal composite anomalies of 500hPa geopotential height, 700hPa geopotential height, 1000-500hPa layer thickness, 700hPa specific humidity, total column precipitable water, and surface air temperature show substantial differences between years with extreme high and low area burned. Considering this, it is reasonable to say that there are special climate conditions that lead to the extremes in area burned. It is important to note that many of the prominent anomalies in the composites for years with

extreme high area burned do not directly correspond with anomalies of the opposite sign for years with extreme low area burned. For example, the positive anomaly centered over Alaska for 500hPa geopotential height for extreme high years in both the preseason and summer does not have a corresponding negative anomaly in the same location during years with extreme low area burned, however the composite anomalies for years with extreme low area burned show a significant positive anomaly south of Alaska instead. This indicates that the climate conditions occurring during extreme high years are not simply just the opposite during extreme low years. Extreme low years generally have their own anomalous synoptic scale situation and extreme high years have their own anomalous synoptic scale situation. This fact implies that there are different mechanisms at work that govern whether or not a fire season in Alaska will have extreme high or extreme low area burned.

Years with extreme high area burned are climatologically characterized by positive height and temperature anomalies either directly over or in the general vicinity of Alaska. These years generally feature a negative anomaly in the height fields present over northwest Russia in the preseason along with a positive anomaly for surface temperature over the Arctic Ocean northeast of Siberia. Positive anomalies are present for all height related climate variables over Alaska during the spring season. In the summer, the height fields tend to show a positive anomaly centered just west of Alaska with a secondary positive anomaly centered over northern Greenland. Surface air temperature has a positive anomaly directly over much of Alaska during the summer.

The placement and signs of the anomalies during the preseason and summer for extreme high years agree with the findings of Henry (1978) who found that there is a correlation between 500hPa geopotential height over Alaska and wildfire occurrence. The results of this study indicate that ridging of long duration occurs during years of high fire occurrence and is shown as a positive anomaly for 500hPa geopotential height (Figure 3.6). This ridging is generally of long enough duration to appear on monthly average composite anomalies of geopotential height. Henry (1978) showed that ridges at 500hPa are present during times of high wildfire occurrence, which agrees with this result. The results of this study further suggest that for an extreme season there is often ridging in place at 500hPa during the preseason as well.

The general climate during the years with extreme low area burned is characterized by a pronounced positive anomaly in the moisture fields over North Africa. This positive anomaly is present throughout both the preseason and during the summer. A hypothesis for the presence of this anomaly is the location of the Intertropical Convergence Zone (ITCZ). It is plausible that the ITCZ was anomalously farther north during the extreme low years examined. The physical relationship between extreme low area burned and the location of the ITCZ over Africa may be purely coincidental however. This is simply because three of the four extreme low years were in sequential order. Examination of the seasonal anomalies for years before and after the set of sequential extreme low years (not shown) revealed that there was a positive moisture anomaly present over the same areas of North Africa starting in the late 1950's until about 1967. This included a positive anomaly for 1957, which is considered in this study

as an extreme high year. Nevertheless, the positive anomaly is present during this period. There is also no positive moisture anomaly in Africa during the summer or preseason for 1978, a season with extreme low area burned also considered, when examined separately (not shown). It is worthy to note that a negative anomaly is present in a similar location for the preseason composite anomalies of moisture for the extreme high years of 2004 and 2005. There is no negative moisture anomaly over North Africa during the summer of any of years with extreme high area burned.

Additional climate features found uniquely during the extreme low years include the presence of a positive anomaly in both the 700hPa and 500hPa geopotential height fields in the North Pacific south of the Aleutian Island chain. In general, this area is the climatological location of the Aleutian Low and may indicate that the low is weaker in this location or shifted farther south as there is a dipole with a positive anomaly to the north and a lesser negative anomaly to the south. There are no significant anomalies in any of the climate variables located over mainland Alaska during the preseason. During the summer period, the lack of significant anomalies over the Alaskan mainland continues for the most part. Overall, it seems that the prevailing climate during the preseason and summer of years with extreme low area burned lacks anomalies of any sign over areas of primary fire occurrence, the mainland portion of Alaska. In fact, as is most notable in Figure 3.15, most significant anomalies occur at lower latitudes for most climate variables in both the preseason and summer. This indicates that the climatological conditions associated with seasons of low area burned during the preseason and summer may in fact be closer to the long-term climatology and not

anomalously different with the main exception of the African moisture anomaly outlined previously.

Altogether, the climate of the preseason and summer of years with extreme low area burned is characterized by anomalies farther away from the center of action of wildfire occurrence. Wildfire occurrence seems to be primarily hindered by the lack of ridging as is seen by the lack of positive height and temperature anomalies as was presented earlier in this section for the extreme high area burned. In contrast, significant positive height and temperature anomalies are present during seasons with extreme high area burned.

4.2 Diagnosing and Predicting Area Burned

The single greatest cause of difficulty in developing the multiple regression models was deciding which and what type of predictor should be considered. As was outlined earlier in the methods section, a good deal of subjectivity was required along with the objective routine for selection. For the preseason and summer, the final set of predictors used for the fitting of the area burned was primarily temperature and moisture climate variables. Most occurred in the months of May and June and were located over Interior Alaska. This time interval of the fire season appears to be of great consequence to the overall area burned during any fire season in Alaska. Overall, geopotential height of the 700hPa level, temperature, and moisture content of the atmosphere over Interior Alaska play major roles during the month of June and are predictors in the final multiple regression. This result is to be expected as temperature and moisture play a strong role

in the occurrence of thunderstorms in the presence of a ridge aloft over Interior Alaska. The lightning from those thunderstorms is the most important ignition source for wildfires with the most of the area burned and as such, is a critical component for the seasonal area burned. Temperature also plays a strong role in the drying of fuels that could be associated with wildfire start and spread. Throughout the entire period, temperature and moisture make up the primary predictors in all months. Outside of the month of June, none of the predictors where located directly over the area where the wildfires in the area burned dataset primarily burn.

Work by Duffy et al. (2005) indicated links between climate conditions before and during the fire season and total seasonal area burned in Alaska. The results of this study agree with the results of Duffy et al. (2005) who, while using a different set of predictors and time period, found an R^2 of 0.79 with seasonal area burned and their fitting. In this study, an R^2 of 0.84 was achieved using the ten climate variables as described previously. The key difference is that a multiple regression only considering the preseason climate conditions was developed as part of this study. This eliminates the need to predict the climate variables in June through August that are required for the spring and summer multiple regression. As a result, this eliminates some of the uncertainty that would be associated with using predicted climate variables in forecasting the area burned when utilizing the multiple regression that considers both spring and summer. The preseason prediction model however, has an R^2 of 0.61, which is lower than either the Duffy et al. (2005) result or the spring and summer multiple regression of this study.

The use of preseason climate variables that have a high correlation with area burned showed itself to be reliable considering the cross validation outcome outlined in the results section. However, the preseason prediction still contains much uncertainty. The three predictors that are part of the preseason multiple regression model fitting have a much more complex relationship with the area burned than the summer predictors as these are farther removed from Alaska in both space and time. There is an apparent relationship between these three climate variables (March 500hPa geopotential height north of India, March 1000-500hPa layer thickness over the Tropical Pacific Ocean, and April column precipitable water over the Arctic Ocean) and the area burned individually. This relation is not simple to diagnose exactly, but is quantified statistically by the multiple regression. From a climate standpoint, it seems likely that these three points are physically related to the seasonal, large-scale circulation as each are associated with large areas of high correlation and/or has multiple climate variables also of high correlation in the same geographic area (see Appendix A). This indicates a complex relationship between these three predictors and the required climate conditions in the summer that control the start and spread of wildfires in Alaska.

When considering the placement, in both time and space, of the preseason predictors, some statement of their physical relationship with the summer fire season can be made. The March predictors could certainly be related to each other in some degree. First, the temperatures over the Tropical Pacific certainly can be related to a shift in storm track that is indicated by the strong 500hPa geopotential height correlation north of India, which is accompanied by an area of negative correlation to the north that was not of large

enough magnitude to be considered as a potential predictor by the scheme used in this study. In April and May there predictors that are related to surface temperature and moisture located geographically north of Siberia over the Arctic Ocean. It seems feasible that the location of the storm track over this part of Asia can impact surface characteristics in these locations by altering snow or sea ice extent. As water has a high heat capacity, this can have a significant impact on temperatures in these regions lasting for months and can certainly influence the weather conditions over Alaska, which is upstream of this geographic area, in the summer. Considering that model performance appears to be best for above average cases, it is reasonable to say that these correlations may be better related to higher than average area burned rather than a general rule for all sizes of fire seasons.

The usefulness of the preseason multiple regression as a predictive tool can certainly be very high, but the problems of the model setup, predictors must be understood to best use this statistical model for making seasonal predictions. This same statement is certainly true of the multiple regression that considers the entire period as well, however, its usage in an operational setting is limited by the need of input data that is from a time in the future and therefore they must also be predicted and hence is also subject to uncertainty.

A potential problem facing the multiple regression fitting is the accuracy of the area burned dataset. Satellite data is not available during the first part of the period of study, so the accuracy of area burned dataset during that period may be biased towards underestimation of area burned. The second, and probably most important effect on the

area burned is the human factor. Humans can strongly influence the amount of area burned by both starting and suppressing wildfires. Both suppression and human caused wildfires occur mostly in the vicinity of the road network, near rivers, and near populated areas. Generally, if a wildfire threatens a populated area in any way, it will be fought extensively. If it happens that an active fire season occurs, but all wildfires start in highly critical suppression areas, the area burned could be reduced from what might have actually occurred. This means that better predictors of area burned could have been missed or skewed to some extent by seasons where good conditions occurred, but wildfires were suppressed.

The NCEP/NCAR Reanalysis dataset encounters some problems that are similar to those that are faced in the early part of the area burned dataset. Accuracy is reduced early on as satellite data was not available, but is used as part of the data assimilation later in the period. The second possible reduction in accuracy is associated with the NCEP/NCAR reanalysis model's dealing of terrain in Alaska. Terrain in the model is lower overall than the topography that is actually present in Alaska. This is a fact that can't be avoided as the model has a grid spacing of 2.5 degrees and mountain ranges have details that require much greater resolution to get an accurate depiction of their true spatial dimensions and detail. Changes in topography from reality to the model can easily alter some of the atmospheric conditions in the model from what might actually be observed.

Other types of climate variables were examined to be potential predictors of area burned besides the ones presented. Many of the studies involving the prediction of

wildfires use drought indices such as the Palmer Drought Severity Index (PDSI). The PDSI along with the Lettau Climatonomy (Lettau 1968) were examined and found to have no statistically significant correlation with the seasonal area burned in Alaska (See Appendix B) and so were not considered viable for use as potential predictors. Sparse data and suspect data quality made the calculation of both of these indices difficult especially considering the entire time period of 1955-2005 for the area burned dataset. It is expected that given improved data for long-term calculation of these drought indices, better correlations might be found with the area burned and this datum could be used as part of the multiple regression or in other methods of prediction and diagnosis. Poor correlations less than 0.4 were also found between area burned and snowmelt date and snow pack amount for Fairbanks. A similar result was found by Butteri (2005) who considered several stations throughout Interior Alaska and found poor correlations with winter precipitation and wildfire occurrence the following fire season.

Having considered the potential inaccuracies in the area burned dataset, problems with predictor selection, etc, now the potentially valuable component of the model can be assessed: operational seasonal prediction. With potential long-term usage of the multiple regression model in mind, it is important to note that the current predictors considered in the model were derived from the set of climate conditions that have occurred during the time period studied. We can assume that the climate controls on the Alaskan fire season, while they may change, should not be so different than those presented in this study given a longer period of time. Nevertheless, the model should be re-calibrated when a longer time series become available and a periodic examination of the predictors as outlined in

the methods section and then refitting the multiple regression based on the new set of potential predictors should be carried out in future. In all, some of the climate variables selected to be predictors might not have been selected had the time period been shorter or longer. Repeating this procedure long term should allow for the statistical model to be "up to date" with the latest climate controls of area burned in Alaska given changes in the overall climate, ecosystems, population density, and changes in fire suppression techniques.

The prediction accuracy assessed for both the spring and summer multiple regression and the preseason multiple regression shows promise especially when trying to predict years that will have particularly high area burned, as in bin 4,050-28,330km^2 of Table 3.5. Both models have a fairly high number of successful predictions for this range of area burned. This demonstrates that these models can be useful in determining if an extreme high year is likely to occur. They may not, however, be as accurate in determining the exact amount of area burned especially for years falling into the range of bins 0-370km^2 to 1,620-4,050km^2 (low to moderate area burned).

Chapter 5 Summary and Conclusions

The climate conditions associated with area burned were examined on the seasonal and monthly scale. Climate variables in the Northern Hemisphere were assessed during the preseason and summer of years with extreme high and low area burned. It was found that years with extreme high area burned tend to have positive anomalies in temperature and height over Alaska during the preseason and summer. Seasons with extreme low area burned tended to lack anomalies of any sign directly over Alaska.

The overall influence of the climate during the preseason and summer on seasonal area burned in Alaska was then quantified using point correlations and multiple regression techniques. Results showed that it is possible to relate the seasonal area burned with only a few climate variables across a few months and located throughout much of the Northern Hemisphere. A critical result was that climate variables in the preseason could be used alone to fit the area burned.

5.1 Extremes Climatology

There are marked differences in the seasonal climatology of atmospheric conditions between years with extreme high and low area burned. In other words, it can be said that there are specific climatological conditions associated with years with high area burned. There is also an identifiable set of seasonal climate conditions that are associated with little or no wildfire occurrence in Alaska. This fact suggests that atmospheric conditions on the monthly and seasonal scale play a critical role in whether

or not a fire season will be of an extreme nature in Alaska. Examination of monthly and seasonal average climate variables can be therefore be a useful tool in assessing the severity of a fire season when considering operational prediction.

Overall, seasons with extreme low area burned are influenced strongly by climatological conditions that are geographically farther away from the areas of wildfire occurrence and are located often at lower latitudes. Seasons with extreme high are burned, however, showed that the atmospheric conditions near or directly over the areas burned during the preseason and summer are significant. Extreme high seasons have a more direct atmospheric anomaly-wildfire relationship.

Wildfires are all strongly influenced by the weather throughout their start and spread. To maintain wildfires of such duration and size so as to have an extreme high season, the climate of the period must be suitable. Seasons with extremely low area burned, while they have generally more climatologically neutral conditions over Alaska, may have atmospheric conditions that are not observable in seasonal composites as they are averaged over when considering a longer period. On shorter time scales, such as monthly or weekly scales, the conditions associated with extreme low area burned may be more discernable. For seasons with extreme low area burned, it is probable that synoptic scale conditions of shorter duration than seasonal scale play a critical role in keeping the amount of area burned to a minimum hence the lack of significant anomalies present over Alaska in the summer seasonal composite anomaly fields.

5.2 Prediction of Area Burned

Predictors selected for fitting area burned occur in greatest number in May and June and are generally located near Alaska during these months as wildfires are ongoing at this time. As was mentioned in the previous section, wildfire occurrence and size is influenced strongly by the weather conditions. May and June are shown to be the most critical time period for determining the total area burned when employing multiple regressions. Outside of May and June during the preseason and later summer, predictors are located farther away geographically from Alaska and show a more teleconnection-like quality. Most of these variables, especially in the preseason, are located upstream of Alaska and suggests influence from the overall, large-scale general circulation.

Most important of all is that it can be concluded from the results of this study that the total seasonal area burned for Alaska climate can be related to scale atmospheric parameters such as 500hPa geopotential height, 700hPa geopotential height, mean sea level pressure, surface air temperature, 1000-500hPa layer thickness, 700hPa specific humidity, and total column precipitable water. This relation shows that there is a critical link between wildfire activity in Alaska and weather and climate. This conceptual link can be quantified by means of statistical models and conceivably put to use as a predictive tool. Assesment of the accuracy of the models to predict different ranges of area burned shows that both models predict area burned relatively well for seasons of exceptionally high area burned. The multiple regression models may not be as effective when considering prediction of exact area burned especially for seasons with near or below average area burned.

5.3 Future Work

Use of multiple regression techniques shows promise as a predictive tool. Considering a longer period for the preseason could improve the accuracy of the forecast made by the multiple regression. An area burned data set broken down by month and by geographic area could be used to develop models that predict area burned during the fire season for more specific geographic areas in Alaska.

The addition of soil moisture and drought indices would be beneficial for the long term prediction of fire seasons. This however requires improvements in the data and area coverage of measurements and long term data sets that do not yet exist for Alaska.

References

Barney RJ (1971) Wildfires in Alaska-some historical and projected effects and aspects. Proceedings of Fire in the Northern Environment-A Symposium. Fairbanks, AK 13-14 April 1971. 51-59

Brotak EA, Reifsnyder WE (1977) An investigation of synoptic situations associated with major wildland fires. J Appl Meteor 16: 867-870

Butteri M (2005) A statistical analysis of the relationship between over-winter snowpack and large fire growth in interior Alaska. Alaska Fire Service

Chambers SD, Chapin FS (2002) Fire effects on surface-atmosphere energy exchange in Alaskan black spruce ecosystems: implications for feedback to regional climate. J Geophys Res-Atmos 108: JD000530

Chu PS, Yan W, Fujioka F (2002) Fire-climate relationships and long-lead seasonal wildfire prediction for Hawaii. In J Wildland Fire 11: 25-31

Crimmins MA (2006) Synoptic climatology of extreme fire-weather conditions across the southeast United States. Int J Climatol 26: 1001-1016

Damoah R, Spichtinger N, Servranckx R, Fromm M, Eloranta EW, Razenkov LA, James P, Shulski M, Forster C, Stohl A (2006) A case study of pyro-convection using transport model and remote sensing data. Atmos Chem Phys 6: 173-185

DeWilde L, Chapin FS (2006) Human impacts on the fire regime of interior Alaska: interactions among fuels, ignition sources, and fire suppression. Ecosystems 9: 1342-1353

Dissing D, Verbyla DL (2003) Spatial patterns of lightning strikes in interior Alaska and their relations to elevation and vegetation. Can J For Res 33: 770-782

Duck TJ, Firanski BJ, Millet DB, Goldstein AH, Allan J, Holzinger R, Worsnop DR, White AB, Stohl A, Diskinson CS, Donkelaar A (2007) Transport of forest fire emissions from Alaska and the Yukon Territory to Nova Scotia during summer 2004. J Geophys Res 112: D10S44

Duffy PA, Walsh JE, Graham JM, Mann DH, Rupp TS (2005) Impacts of large-scale atmospheric-ocean variability on Alaskan fire season severity. Ecological Applications 15: 1317-1330

Fauria MM, Johnson EA (2006) Large-scale climatic patterns control large lightning fire occurrence in Canada and Alaska forest regions. J Geophys Res 111: G04008

Flannigan MD, Harrington JB (1987) A study of the relation of meteorological variables to monthly provincial area burned by wildfire in Canada (1953-80). Journal of Applied Meteorology 27: 441-452

French NHF, Kasischke ES, Williamas DG (2003) Variability in the emssion of carbon-based trace gases from wildfire in the Alaskan boreal forest. J Geophys Res 108: 8151

Henry DM (1978) Forecasting fire occurrence using 500mb map correlation. NOAA Technical Memorandum, NWS AR-21: 31 pp

Hess JC, Scott CA, Hufford GL Fleming MD, (2001) El Nino and its impact on fire weather conditions in Alaska. Int J Wildland Fire 10: 1-13

Hostetler SW, Bartlein PJ, Solomon AM, Holman JO, Busing RT, Shafer SL (2005) Climatic controls of fire in the western United States: from the atmosphere to ecosystems. Joint Fire Sciences Program Report 01-1-6-05

Johnson EA, Wowchuck DR (1992) Wildfires in the southern Canadian Rocky Mountains and their relationship to mid-tropospheric anomalies. Can J For Res 23: 1213-1222

Kalnay EM, Kanamitsu R, Kistler W, Collins D, Deaven L, Gandin M, Iredell S, Saha G, White J, Woollen Y, Zhu A, Leetmaa B, Reynolds M, Chelliah W, Ebisuzaki W, Higgins J, Janowiak K, Mo C, Ropelewski J, Wang R, Joseph J, Joseph D, (1996) The NCEP/NCAR 40-year reanalysis project. Bull Amer Meteor Soc 77: 437–471

Kasischke ES, Williams D, Barry D (2002) Analysis of the patterns of large fires in the boreal forest region of Alaska. Int J Wildland Fire 11: 131-144

Lettau H (1969) 1. A new approach to numerical prediction of monthly evapotranspiration, runoff, and soil moisture storage. Mon Wea Rev 97: 691-699

Lynch JA, Hollis JL, Hu FS (2004) Climatic and landscape controls of the boreal forest fire regime: Holocene records from Alaska. J Ecology 92: 477-489

McGuiney E, Shulski M, Wendler G (2005) Alaska lightning climatology and application to wildfire science. Proceedings of the Conference on Meteorological Applications of Lightning Data. 9-13 January 2005. American Meteorological Society

Mölders N, Kramm G (2007) Influence of wildfire induced land-cover changes on clouds and precipitation in interior Alaska - a case study. Atmospheric Research 84: 142-168

Pereira MG, Trigo RM, Camara CC, Pereira JMC, Leite SM (2005) Synoptic patterns associated with large summer forest fires in Portugal. Agr Forest Meteor 129: 11-25

Potter BE (2002) A dynamics based view of atmosphere-fire interactions. Int J Wildland Fire 11: 247-255

Pyne SJ, Andrews PL, Laven RC (1996) Introduction to wildland fire, second edition. John Wiley & Sons, Inc. 769 pp

Reap RM (1991) Climatological characteristics and objective prediction of thunderstorms over Alaska. Weather and Forecasting 6: 309-319

Searby HW (1968) Climates of the states: Alaska, climatography of the United States No. 60-49. U.S. Department of Commerce

Schaefer VJ (1957) The relationship of jet streams to forest wildfires. J Forestry 55: 419-425

Schroeder MJ, Glovinsky M, Hendricks VF, Hood FC, Hull MK, Jackobson HL, Kirkpatrick R, Krueger DW, Mallory LP, Oertel AG, Reese RH, Sergius LA, Syverson CE (1964) Synoptic weather types associated with critical fire weather. Pacific Southwest Forest and Range Experiment Station, Berkeley CA. 492 pp

Skinner WR, Stocks BJ, Martell DL, Bonsal B, Shabbar A (1999) The association between circulation anomalies in the mid-Troposphere and area burned by wildland fire in Canada. Theor Appl Climatol 63: 89-105

Skinner WR, Flannigan MD, Stocks BJ, Martell DL, Wotton BM, Todd JB, Mason JA, Logan KA, Bosch EM (2001) A 500hPa synoptic wildland fire climatology for large Canadian forest fires, 1959-1996. Theor Appl Climatol 71: 157-169

Sullivan WG (1963) Low-level convergence and thunderstorms in Alaska. Mon Wea Rev 91: 89-92

The Alaska Climate Research Center (2007). http://climate.gi.alaska.edu.

The NCEP/NCAR Reanalysis Project at the NOAA/ESRL, Physical Sciences Division (2006). http://www.cdc.noaa.gov/cdc/reanalysis.

Trouet V, Taylor AH, Carleton AM, Skinner CN (2006) Fire-climate interactions in forests of the American Pacific coast. Geophys Res Let 33: L18704

Westerling AL, Cayan DR, Gershunov A, Dettinger MD, Brown T (2001) Statistical forecast of the 2001 western wildfire season using principal components regression. Experimental Long-Lead Forecast Bulletin 10: March 2001

Westerling AL, Gershunov A, Bronw TJ, Cayan DR, Dttinger MD (2003) Climate and wildfire in the western United States. Bull Amer Meteor Soc 84: 595-604

Wilks DS (2006) Statistical methods in the atmospheric sciences, second edition. Burlington, MA. Elsevier Academic Press Publications. 627 pp

Appendix A

A result of the predictor selection process outlined in section 2.2.3 was a series of point correlations for the Northern Hemisphere for each month for each climate variable. Here we show the correlation plots that contain the predictors used in the spring and summer multiple regression (Table 3.2) and the predictors used for the preseason multiple regression (Table 3.4). This gives an idea as to the spatial size and shape of the area of correlation that each predictor represents.

The three predictors used in the preseason multiple regression (Table 3.4) where chosen from the correlation fields depicted in Figures A.1, A.2, and A.3. In Figure A.1, the predictor was located in the area of high positive correlation centered generally over the northern tip of India and is accompanied by an area of negative correlation to the north. The second predictor used by the model was associated with the area of high positive correlation located in the Pacific Ocean near the Equator in Figure A.2. The final figure was taken from the near center of the bull's eye of high correlation located in the Arctic Ocean northeast of Siberia in Figure A.3.

The 10 predictors used in the final model for the spring and summer multiple regression (Table 3.2) were taken from the correlation fields of Figures A.3 through A.9. The first predictor was selected from the 700hPa specific humidity field, which has a virtually identical field to Figure A.3, so is not shown. As was the case with the preseason predictor from the April total column precipitable water field, the 700hPa specific humidity predictor for April used by the spring and summer multiple regression was taken from the same location northeast of Siberia. The April surface temperature

predictor is located in the same geographic location as the total column precipitable water predictor (not shown).

The moisture correlation fields for May were both nearly identical to Figure A.4 (therefore one is shown). Two predictors were selected from this field: one was associated with the area of high positive correlation over the Arctic Ocean, and the second was associated with the area north of and including the Aleutian Islands. The 1000-500hPa layer thickness predictor for May (Figure A.5) was located in the Gulf of Alaska with the area of positive correlation located right on the southern coast of Alaska.

In June, as shown in Figures A.6 and A.7, predictors were located in areas of high positive correlation with area burned over interior Alaska. In August, the surface air temperature predictor was located in the Bering Sea associated with an area of high positive correlation covering much of the southern Bering Sea (Figure A.8). The second August predictor was related to the area of high correlation in the central Pacific in Figure A.10.

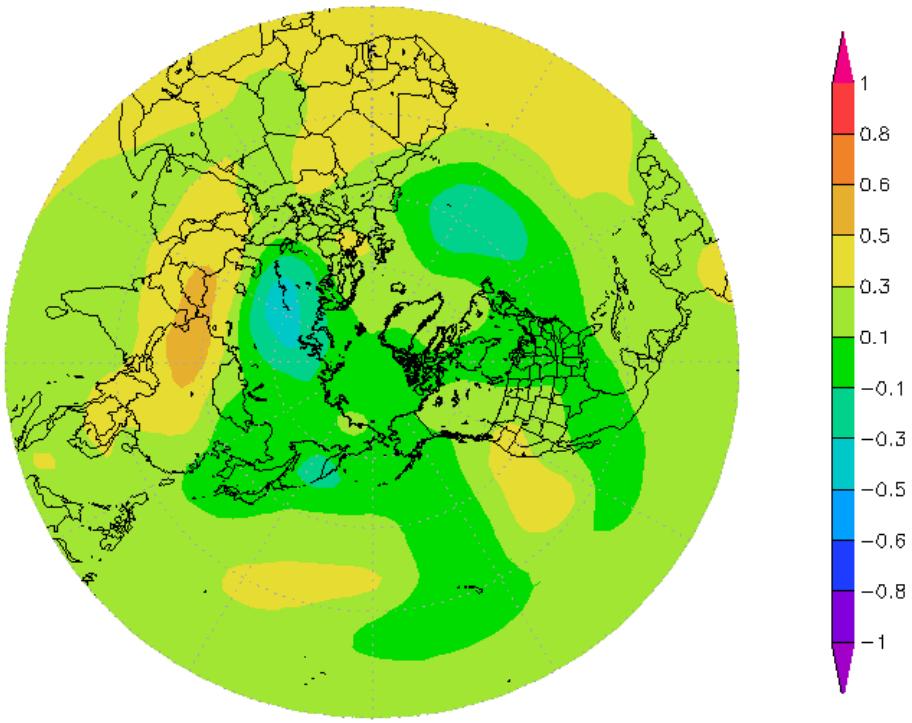

Figure A.1 Point correlations of seasonal area burned with March 500hPa geopotential height.

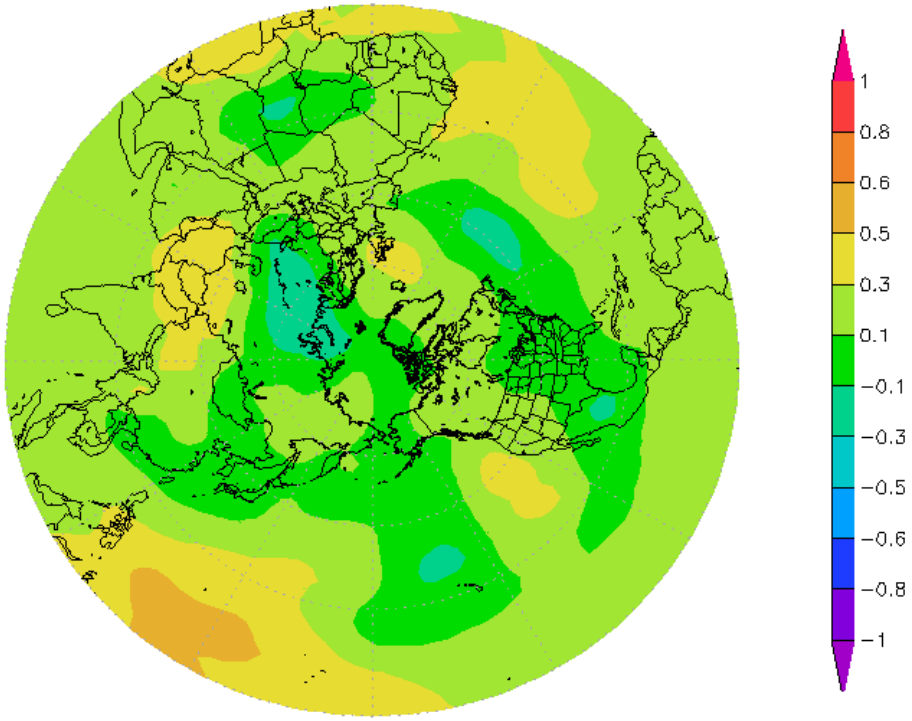

Figure A.2 Point correlations of seasonal area burned with March 1000-500hPa layer thickness.

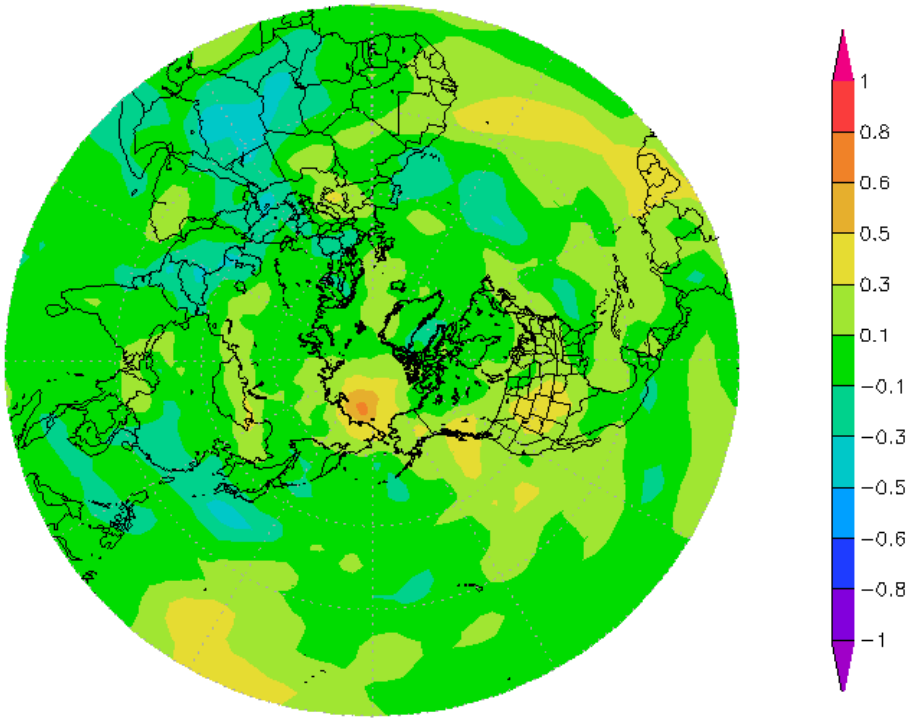

Figure A.3 Point correlations of seasonal area burned with April total column precipitable water.

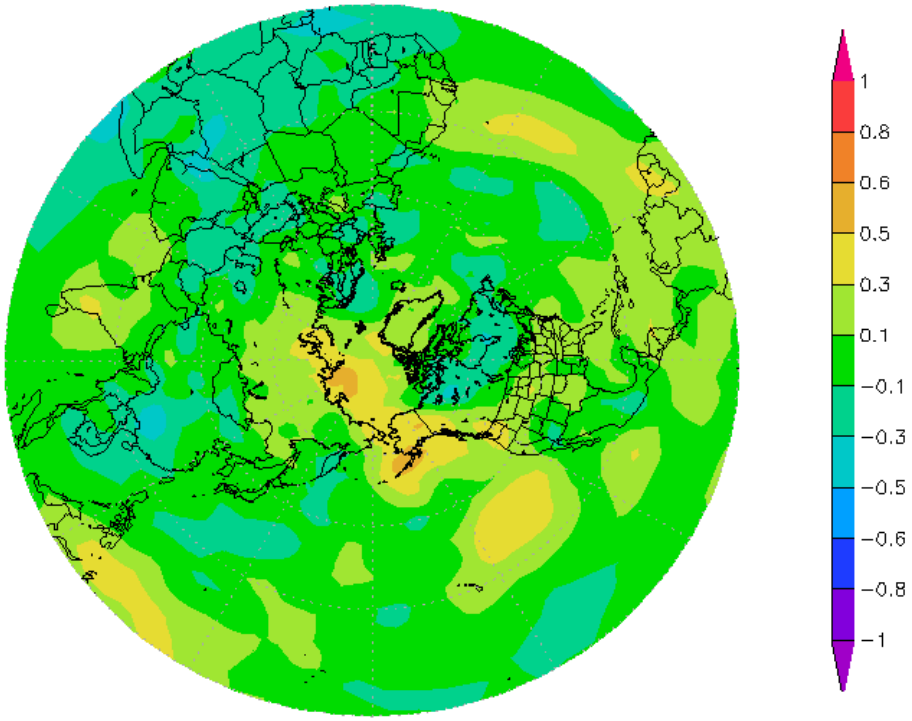

Figure A.4 Point correlations of seasonal area burned with May total column precipitable water.

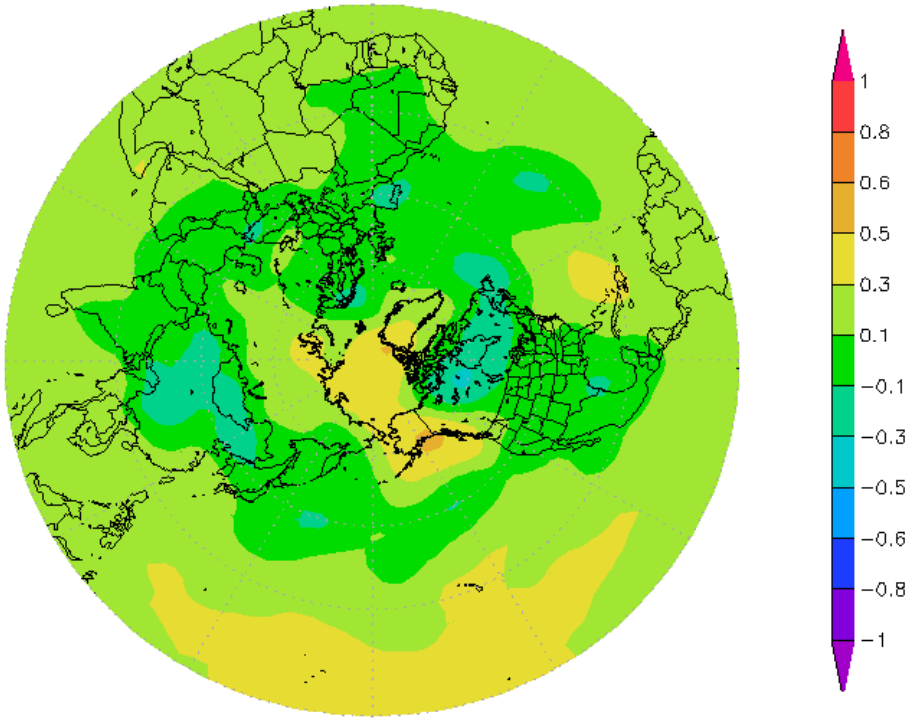

Figure A.5 Point correlations of seasonal area burned with May 1000-500hPa layer thickness.

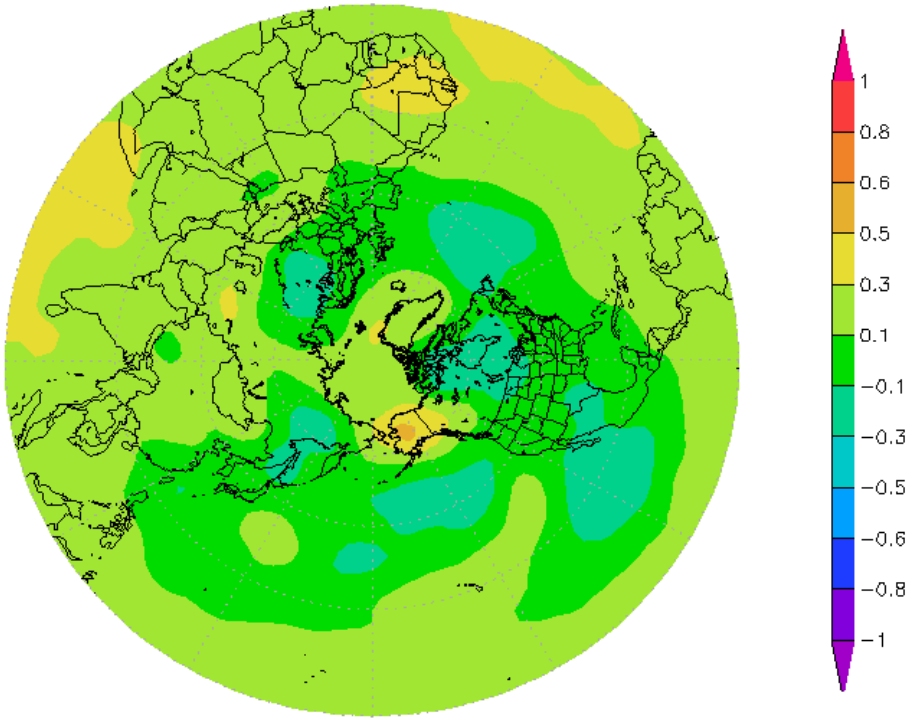

Figure A.6 Point correlations of seasonal area burned with June 700hPa geopotential height.

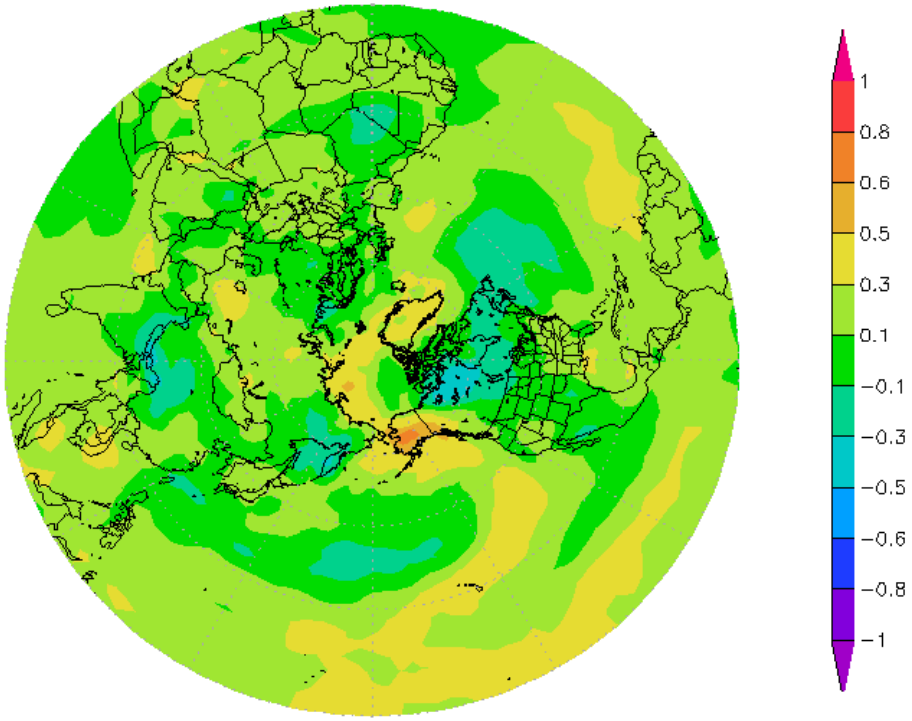

Figure A.7 Point correlations of seasonal area burned with June surface air temperature.

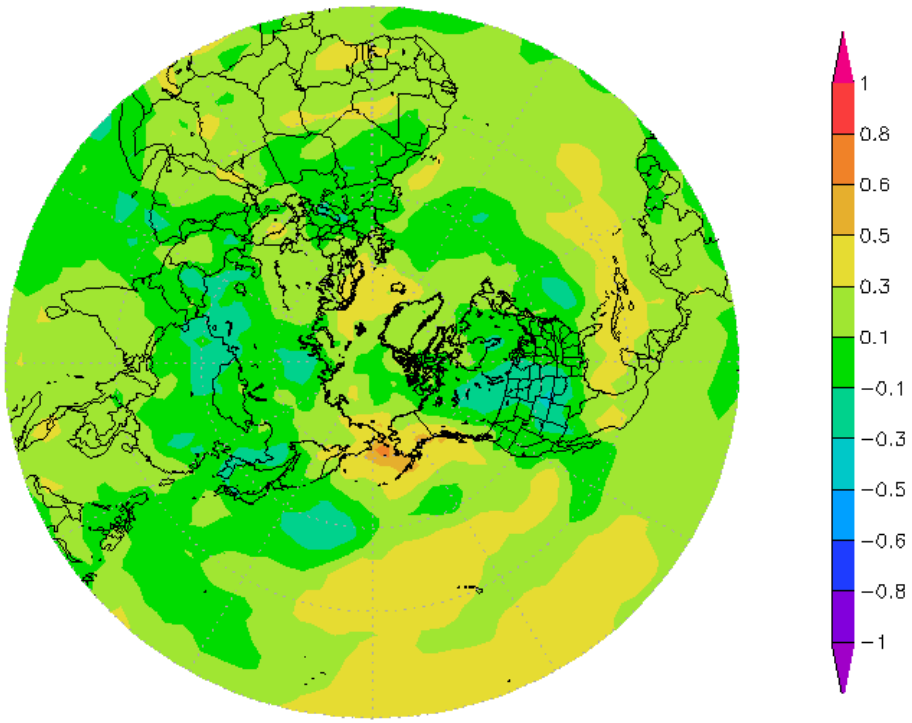

Figure A.8 Point correlations of seasonal area burned with August surface air temperature.

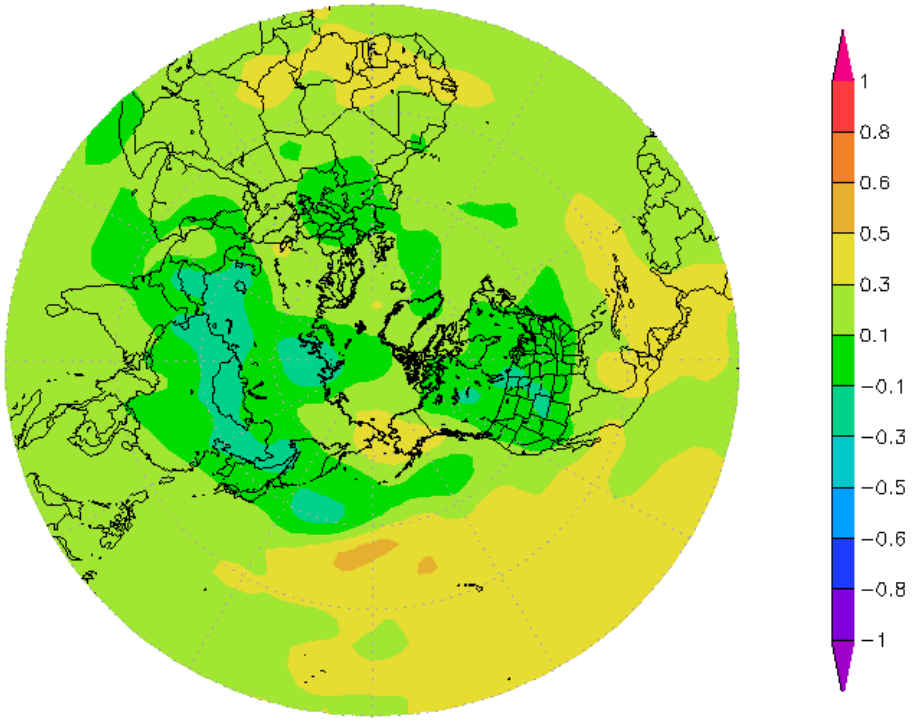

Figure A.9 Point correlations of seasonal area burned with August 1000-500hPa layer thickness.

Appendix B

In an effort to determine what types of variables would be useful in predicting area burned in Alaska, a few drought indices were examined. The index examined for this study was the Lettau Climatonomy (Lettau 1969). This index is based on a fairly simple, yet highly physical formula:

$$LE = (1 + Bo) * (1 + Ro / P) \quad \text{(B.1)}$$

Where Bo is the Bowen Ratio, and the runoff ratio Ro/P is Ro as the runoff, and P as the precipitation. Equation B.1 results in a dryness index value LE for the Lettau Climatonomy.

For this study, monthly average values for the Bowen Ratio from an instrument tower in the Caribou Poker Creeks Research Water Shed (CPCRWS), which is associated with the University of Alaska Fairbanks, were used. Data from the CPCRWS was taken from towers labeled C4MET and CRREL. Unfortunately, the data for these towers begins in 1998 therefore average values of monthly average Bo were used for the long term LE for the entire period. This was one of the major sources of difficulties that likely contributed to the low correlations that resulted. Another problem was that there appeared to be errors in the data such so the suspect values were then thrown out of our calculation of the long term average Bo that was used in the final calculations. These factors greatly shortened the available amount of Bo observations that could be considered for the LE calculation.

Monthly total accumulated precipitation for Fairbanks was obtained for the Fairbanks International Airport station for the period 1955-2005. Monthly accumulated runoff was calculated from a United States Geological Survey stream gauge that measures stream flow of Chena River from the Chena Basin. These data were used in conjunction with the calculated monthly average Bowen Ratio in Equation B.1 to calculate monthly average values of LE for the months of the fire season (Figure B.1).

When correlated with total seasonal area burned dataset, correlations were negative, but of very low magnitude. The highest correlation of monthly LE with seasonal area burned was -0.43 for August. May through June had correlations less than 0.2. It seems probable that these correlations could be improved given a long term dataset from which Bowen Ratio could be calculated. It is also important to note that this calculation was only carried out for Fairbanks observations and not for other stations in Alaska due to the lack of data (especially radiation budget data). It is possible that LE calculated from other stations could also produce improved values of correlation.

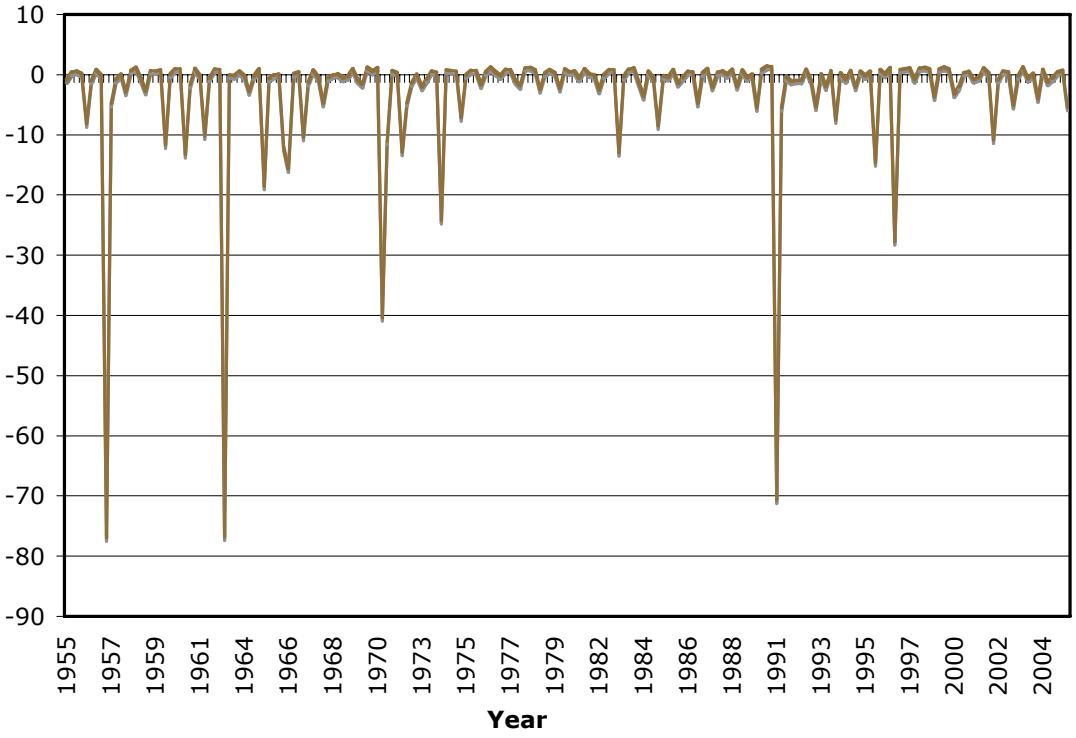

Figure B.1 May, June, July, and August dryness index for the Lettau Climatonomy (LE) calculated from Equation B.1.